

Anatomic Variation of the Knee Extensor Mechanism: The Effect on Tibiofemoral Joint Load and Joint Kinematics

By

Nicholas J. Riggert

Submitted to the graduate degree program in Bioengineering and the Graduate Faculty of the University of Kansas in partial fulfillment of the requirements for the degree of Master of Science.

Dr. Lorin Maletsky, Chairperson

Dr. Lisa Friis, Committee Member

Dr. Sara Wilson, Committee Member

Date Defended: July 11, 2017

The Thesis Committee for Nicholas Riggert certifies that this is the approved version of
the following thesis:

Anatomic Variation of the Knee Extensor Mechanism: The Effect on Tibiofemoral Joint
Load and Joint Kinematics

Chairperson Dr. Lorin Maletsky

Date Approved: _____

Abstract

Background: Variation to extensor mechanism features of patella thickness, patella height, and tuberosity AP (anterior-posterior) and SI (superior-inferior) position will effect knee kinematics and tibiofemoral (TF) joint loads. The variations primarily relate to alterations of the patellar ligament angle, relative to the long axis of the tibia. There are two objectives in this study, first, determine the desired setting of each feature within the analog configuration of the Kansas Knee Simulator (KKS) to better match measured in-vitro TF-AP loads. Second, to describe the correlations between the features, quadriceps load, TF kinematics and patellofemoral (PF) kinematics

Methods: To determine the desired analog configuration in the KKS, a custom instrumented tibia tray (ITT) was assembled with total knee replacement components from DePuy Synthes (Attune Primary, Size 8). The ITT measures TF joint load while simulating a dynamic walk and squat motion in the KKS. A design of experiments (DOE) was established, using the Taguchi analysis method to minimize the calculated RMS error. Each feature was varied between three levels. All experiments were conducted in a random order in three separate trials. To determine kinematic correlations between features, a different simulated walk was applied to 18 fresh frozen cadaver knees (age 59.3 ± 13.2 years old, 25.1 ± 6.4 BMI) in the KKS. Data points were taken at every 5% of the cycle for quadriceps load, and TF and PF kinematics. The data were normalized to create an 18x151 correlation matrix for principle component (PC) analysis. Subsequent PCs were included for analysis until 80% total explained variation was reached. The resulting coefficient matrix (“loadings”) was used to show the correlation between variables for each PC.

Results: Signal-to-noise ratios for each feature were used to set the desired analog configuration at a patella thickness of 28.3-mm, patella height of 44.4-mm, and a tuberosity position of 29.3-mm (SI) and 40.6-mm (AP). The desired configuration reduced the calculated RMS error from 71.95-lbs in the

original configuration to 4.76-lbs. The most sensitive factors affecting TF-AP load are patella thickness and tuberosity position. The PC analysis found the first 5 PCs accounted for over 80% of the variation. PC-1 explained 33.4% of the total variation and shows a correlation of patella height to changes in a majority of kinematic descriptions included in this analysis. The remaining PCs showed correlations to specific kinematics and anatomic measures at decreasing amounts of explained variation.

Conclusion: Patella thickness and tuberosity position, and the corresponding patella ligament angle, have the greatest effect on TF-AP load. These measures are associated with minimal explained variation and correlated to limited kinematic changes. Patella height had minimal effect on TF-AP load, but is associated with the majority of explained variation and correlated to changes in quadriceps load, tibia rotation, and patella spin, tilt, and ML translation. TF-AP load is most affected by variation in patella thickness and tuberosity position, and kinematic changes are most affected by variation in patella height. Understanding the effects of variation in the three extensor mechanism features will guide more informed conclusions in future research, prosthetic and surgical tool development, and decisions regarding medical intervention.

Table of Contents

Abstract.....	iii
Acknowledgements.....	ix
1. Introduction	1
2. Literature Review.....	3
2.1. Patella Thickness.....	4
2.2. Joint Line Elevation	8
2.3. Tibia Tuberosity Location.....	13
3. Effect of Variability of Extensor Mechanism Features on kinematics and Tibiofemoral anteroposterior loads	18
3.1. Introduction and Background	18
3.2. Materials and Methods.....	21
3.2.1. Tibiofemoral AP Load Evaluation	23
3.2.2. Kinematic Evaluation.....	25
3.3. Results.....	32
3.3.1. Tibiofemoral AP Load Evaluation	32
3.3.2. Kinematic Evaluation.....	33
3.4. Discussion.....	34
3.4.1. Tibiofemoral AP Load Evaluation	34
3.4.2. Kinematic Evaluation.....	37
3.5. Conclusion.....	41
3.6. Future Work.....	44
Appendix A: Kansas Knee Simulator LabView control system.....	46
A1. Introduction and Background	46
A2. Labview System and Methods	47
A3. Results and Discussion	50
A4. Conclusion and Future Controls Work.....	51
Appendix B: Additional Figures.....	56
References	70

List of Figures

Figure 1: (Left) - Kansas Knee Simulator (KKS) with cadaver specimen under dynamic simulation. This figure shows the sagittal plane actuators (vertical load, ankle flexion moment, and quadriceps hip flexion). Motion from each actuator affects the others and influence flexion. The quadriceps load is free to change and is a result of the applied ankle and vertical actuator loads to achieve targeted flexion. (Right) – Shows the analog configuration and out of sagittal plane actuators (Internal-External torque and Adduction-Abduction moment)..... 28

Figure 2: ITT Sensor used in DOE trials, with the lateral tibia insert removed to reveal the underlying lateral load cell. The insert shown is a DePuy Attune Primary implant, size 8..... 29

Figure 3: Dynamic simulation input profiles for KKS sagittal plan actuators. Plots on the left show actuator targets for walk profiles WalkCAD (used to evaluate natural knee kinematics) and WalkDOE (used to evaluate TF-AP loads). Plots on the right show the Simple Squat input profile actuator targets that were also used to evaluate TF-AP loads. Target loads are in pounds. Hip angle target is assuming that it is half of the TF flexion angle, so peak angle shown in the quadriceps actuator for the squat at 55° would correspond to a TF flexion angle of 110° at peak flexion. This assumes that the tibia and femur are identical lengths from the FE axis of rotation..... 30

Figure 4: Grood-Suntay PF coordinates system and directions, as represented on a left knee. The same directions are applied to tibiofemoral kinematic descriptions, with the SI axis along the long axis of the tibia. The floating axis represents the AP axis, and SI movement is described as displacement from the femoral origin along the fixed body SI axis of the tibia/patella, and ML movement is along the flexion axis along the epicondylar width of the femur..... 31

Figure 5: Physical set-up of analog components in the KKS. The components being used for this experiment are Primary Attune (DePuy Synthes), Sz 8. Patella height and tibia tuberosity position measurements are made from an origin located on the tibia plateau at the midpoint between the medial and lateral tibia condyles. Patella thickness is altered using fixed width inserts placed between the patella composite and the Kevlar strap (representing the patellar ligament). 32

Figure 6: Taguchi Response plot of each factor and level. This shows the average signal-to-noise ratio for the normalized RMS error of AP load between experimental and Cadaver Target AP loads from all three experimental trials. The maximum SN ratio of each factor identifies the level that minimizes the RMS error and corresponds to the desired level for each factor. 36

Figure 7: Improvement in achieving Cadaver Target AP loads with the new, desired configuration determined from the DOE, compared to the old analog configuration for the WalkDOE profile. RMS error of total AP load decreased from 71.95 lbs to 4.67 lbs..... 37

Figure 8: Walk Profile scree plot of both individual PC and total explained variation. Subsequent PCs are used for analysis until a threshold of 80% total explained variation is reached. This plot shows that including the first five PCs will achieve 80% total explained variation and are the only PCs used in the analysis..... 40

Figure 9: Walk Profile - PC1 (described 33.38% of data variation). Plot includes all variables of the mean and after perturbing PC1 by ± 3 standard deviations. The coefficients for each variable are color coded along mean data line (blue colors are negative coefficients, red colors are positive coefficients). Bright

red and dark blue represent strong correlations (70% of max/min) and magenta and light blue represent weak correlations (50%-69% of max/min). Quadriceps load is shown in the upper left corner, TF IE rotation is middle-top and TF AP translation is upper-right corner. The bottom 4 plots are PF kinematics, FE, VV, IE, and ML motion from left to right, top to bottom respectively. The geometric measurements of patella height, patella thickness, and tuberosity position are shown in the lower left corner. The same plot configuration was used for the four remaining PCs included in the analysis. 41

Figure 10: Process Flow Diagram of KKS Controller Utilized in LabView Code. The red boxed components show the cross compensation algorithm used for the vertical load and ankle load actuator. 53

Figure 11: KKS Actuator Tracking Performance using the LabView cRIO system and cross compensation (after filtering sensor signal) applied to the vertical load and ankle load actuators. The profile being tracked is the 'WalkDOE' profile utilized in the TF-AP load evaluation. 54

Figure 12: KKS actuator tracking ability using the Instron system. The sensor signals have not been filtered here and the tracking data had to be cut, resampled, and overlaid with the target data. This is due to the tracking data not being recorded at consistent intervals compared to the input target data. This shows the tracking for the “WalkDOE” profile that was used in the TF-AP load evaluation. 55

Figure 13: (LEFT) Location of tuberosity positions (sagittal plane, anterior to the left) on the analog fixture relative to the center of the tibia insert. Locations are related to a Sigma total knee replacement sizes that correlate to a certain anatomical sized knee. (i.e. size 2 would be a smaller knee than size 6 and have a more posterior and superior tibia attachment position relative to the center of the tibial plateau). (RIGHT) Isometric view of the KKS fixture assembly using the load cell. In these figures, the blue load cell and top plates can be replaced with the ITT and still work. 56

Figure 14: The variable tuberosity positions compared to the original configuration attachment position (blue hole). The associated holes in the above figure are 1.5 (upper right), 2 (upper left), 5 (lower left), and 4 (lower right). To utilize the attachment sites on the left, the attachment fixture would need to be rotated so that sizes 2 and 5 would be closer to the tibia plateau (i.e. only holes on right can be used for tibia attachment positions). 56

Figure 15: Average total Anterior (+) / Posterior (-) loads of all 9 experiments from the DOE for the “WalkDOE” profile among all 3 trials run. Standard deviation of all the trials is reported every second. The low standard deviation suggests good repeatability between all trials for every experiment with the most deviation occurring in swing phase (the last 4 seconds). 57

Figure 16: Average total Anterior (+) / Posterior (-) loads of all 9 experiments from the DOE for the “Simple Squat” profile among all 3 trials run. Standard deviation of all the trials is reported every second. The low standard deviation suggests good repeatability between all trials for every experiment. 58

Figure 17: Average SI compressive forces from all trials of the 9 experiments (dashed lines) for the “WalkDOE” profile. Minimal variation between experiments and trials can be observed. The Cadaver Target data (black) and the desired configuration (green) show good comparison, therefore the desired configuration did not negatively impact SI compressive force. 59

Figure 18: Average AP loads during the “WalkDOE” profile for all 3 trials including the result of the desired configuration setting (green). 60

Figure 19: Walk Profile - PC2 (20.51% explained variation). 61

Figure 20: Walk Profile - PC3 (12.87% explained variation).	61
Figure 21: Walk Profile - PC4 (8.97% explained variation).	62
Figure 22: Walk Profile - PC5 (5.74% explained variation). After this PC, more than 80% of variation in original data was explained.	62
Figure 23: Trial 3 offset TF kinematics for all 9 DOE experiments. Single profile of WalkDOE walk cycle.	63
Figure 24: Trial 3 offset PF kinematics for all 9 DOE experiments. Single profile of WalkDOE walk cycle.	64
Figure 25: Trial 3 offset quadriceps load measured during a single cycle of the WalkDOE walk profile for all 9 DOE experiments.....	65
Figure 26: Natural knee offset TF Kinematics of a single WalkCAD walk profile for all 19 knees considered in PC analysis. The red line that varies considerably in the AP translation plot (middle, bottom) is knee number 11 and is considered an outlier and omitted from the PC analysis.	66
Figure 27: Natural knee offset PF Kinematics of a single WalkCAD walk profile for all 19 knees considered in PC analysis. The same outlier identified in natural knee TF kinematics is removed from the PF data set for PC analysis as well.	67
Figure 28: Natural knee offset measured quadriceps load of a single WalkCAD walk profile for all 19 knees considered in PC analysis.....	68
Figure 29: PC1 vs. PC2 scores of the 18 original observations included in the PC analysis of the natural knees (black) plotted against the scored DOE kinematics and quadriceps load (green). The variation of the DOE kinematic data was much narrower than the cadaver kinematic data; however, these two data sets were conducted with different profiles, under different considerations, comparing TKA components and natural knee structures. It is expected that the DOE data will not have the same spread as the anatomic data.	69

List of Tables

Table 1: DOE Factors and the settings of all three levels for each.	24
Table 2: DOE factor sensitivity for walk and squat profiles, and peak SN ratios.	33
Table 3: PC correlation summary and percent explained variation of each PC. Fields with \pm are variables with coefficients $> 70\%$ of the maximum value, representing strong correlations. Fields with (\pm) are variables with coefficients $>50\%$ and $<70\%$ of the maximum value, representing weak correlations. No symbol indicates no correlation. Similar signs show variables are correlated in the same direction where opposite signs show variables correlated in opposite directions. The results are shown for the first five PCs only.	34
Table 4: Load control PID tuning values for all actuators	48
Table 5: Position control PID tuning values for all actuators for those with active position sensors.	49
Table 6: KKS Cross-Coupling Coefficients for the vertical and ankle actuator.....	49
Table 7: KKS Cross-Coupling PID values for the ankle actuator signal.....	50
Table 8: KKS Tracking performance, percent normalized RMS error between the cRIO and Instron control system	51
Table 9: DOE Experimental Array corresponding to results obtained in this study.	57

Acknowledgements

My personal journey to completing this thesis would not be possible without the support of my fiancée, Nikki, and deserves more than these words can offer. She had to deal with me leaving for Kansas while she remained in Houston immediately following our engagement. She has been a constant source of support and has shown great patience, enduring the long periods we have been away from each other. I owe so much to her and cannot thank her enough for the sacrifices she has made in order for me to achieve my goals.

I must also thank my advisor, Dr. Lorin Maletsky for his constant guidance and support throughout my investigation. The freedom to explore this topic and to have provided me with such a great opportunity has made me a better engineer than I imagined I could be. I also owe my success and the completion of this thesis to all past and current members of the Engineering Joint Biomechanics Research Lab, most notably Matthew Dickenson, Bardiya Akhbari, and Fallon Fitzwater.

List of Abbreviations

ML	Medial-Lateral Translation
AP	Anterior-Posterior
SI	Superior-Inferior
IE	Internal-External
VV	Varus-Valgus
FE	Flexion-Extension
TF	Tibiofemoral
PF	Patellofemoral
KKS	Kansas Knee Simulator
PC	Principal components
TKA	Total knee arthroplasty
DOF	Degrees of freedom
DOE	Design of Experiments
ITT	Instrumented tibia tray

1. Introduction

The extensor mechanism of the knee is one of the most functionally important structures of the knee. The main purpose of the mechanism is to control flexion-extension of the tibia relative to the femur during quadriceps contraction. This mechanism incorporates three bones of the knee, the femur, patella, and tibia. Extension of the knee is produced by the contraction of the quadriceps, pulling on the tendon at the proximal end of the patella. The load is transferred to the patellar ligament that connects the patella to the tibia. All of these individual structures combine to form the complete extensor mechanism.

Two characteristics of the femur play a role in the extension of the knee. First, the geometry and sagittal-plane shape of the condyles (known as the J-curve) determines the axis of flexion rotation. In deep flexion the rotation axis moves posterior on the tibia allowing for a greater moment arm creating a larger mechanical advantage. Second, the geometry of the trochlear groove keeps the patella engaged and constrained medially and laterally as flexion angle increases. This ensures that the line of action of the quadriceps remains consistent as the knee flexes and keeps the patella from dislocating laterally. The importance of this function is highlighted in patients with femoral dysplasia, where the trochlear groove is not able to maintain proper tracking of the patella, causing pain and frequent patellar dislocation.

The primary function of the patella is to provide an articulating surface against the femur and to provide a moment arm relative to the FE axis of rotation. The conforming geometry of the posterior cartilage to the femoral trochlear groove maintains proper patellar tracking. The thickness of the patella is also important as this changes the length of the moment arm across flexion ranges. A thicker patella has been shown to provide a greater mechanical advantage in deep flexion, thus reducing the required quadriceps force to extend the tibia [1][2][3][4].

The role of the tibia in relation to the extensor mechanism is to provide an insertion point for the patellar ligament. The location of this insertion point is known as the tibia tubercle. Typically the tubercle lies slightly lateral, anterior, and distal to the anterior tibial plateau. The exact position of the tuberosity relative to the tibial plateau, femur and patella can greatly affect the kinematics of the extensor mechanism [5][6][7][8][9][10]. The relationship between the tuberosity position and the patella will affect the angle of the patellar ligament and line of muscle action which can affect patellar kinematics and total joint loads.

The soft tissue structures play an important role as well. There are four different quadriceps muscles that act on the proximal edge of the patella to extend the knee. These muscles are the rectus femoris, vastus medialis, vastus lateralis, and vastus intermedius. The vastus lateralis and vastus medialis can be further reduced to the vastus obliquus and vastus longus, making a total of six defined muscle groups whose distal fibers all attach to the proximal patella [11]. These different muscle groups all combine to affect the patellar kinematics [12], and it has even been shown that a weak vastus medialis obliquus can be an indicator for patients with a high risk of patellar dislocation. The patellar ligament is important, as the fixed length of the structure and its insertion point on the tibia tuberosity can affect the patella height and patellar ligament angle. The two factors can affect overall joint load and have been used as an indicator in patellar dislocation.

In the current Kansas Knee Simulator (KKS) analog component configuration there is a single tuberosity attachment site, a single patella thickness, and the patella is positioned high on the femur. While operating the KKS in this configuration, high anterior loads are generated which don't match targeted physiologic loads. Initial changes included moving the tuberosity attachment both superior-inferior (SI) and anterior-posterior (AP), and altering the patella height. These initial changes to the configuration resulted in altered AP loads, but did not approach physiologic loads. Therefore, cadaver specimens are currently used in order to generate KKS actuator profiles that replicate natural joint

loads. This method is time consuming, difficult, and requires the cadaver specimen to endure rigorous loading. By determining what parameters affect AP loads a more accurate physiological match using analog knee fixtures may be obtained. This would allow KKS actuator profiles to be generated with analog components and be completed in a timely and cost effective manner.

There are two main objectives of this thesis. The first is to assess the extensor mechanism factors in the analog configuration of the KKS that affect AP joint loads, to better replicate physiological tibiofemoral (TF) joint loads for future cadaver studies. The second objective is to assess how the same factors change within the natural morphology and their effect on quadriceps load, patellofemoral (PF) and TF kinematics.

This thesis is broken into several different chapters. The first chapter is a literature review that discusses the three factors of the extensor mechanism that were focused on in this study, patella thickness, patella height (joint line elevation), and the tibia tuberosity location. The second chapter discusses the methods and results laid out in a manuscript format for future publication. The appendix discusses the custom LabVIEW code created to control the KKS and its relation to the performance with the Instron system, and includes additional figures relating to the results of this study.

2. Literature Review

This review focuses on the effect of three anatomic features of the extensor mechanism: patella thickness, patella height (i.e. joint line elevation), and tibia tuberosity position (i.e. insertion point of the patellar ligament on the tibia). There are two parts to this review for each feature; the effect of changes on kinematics and kinetics, and the surgical options that will vary the given feature.

Post-surgical failures of TKAs leading to revision are becoming less frequent but remain a concern and are potentially harmful. While previous studies have reported infection being the leading cause for revision, they often fail to distinguish between early life vs late life failure rates for implants [13].

Studies that account for failure rates at different stages of component lifecycle note that aseptic loosening is the most common cause for revision and remains fairly consistent throughout implant lifecycle (23.1% - 31.2%) followed by infection, wear and instability. In early life (< 5years) infection is most common (23% - 30%) and instability is second (24% - 25%) [14][15]. The cause for these failures is generally multifactorial and difficult to define. Instability and loosening have been attributed to poor gap balancing, component malpositioning, ligament insufficiency, extensor mechanism insufficiency, implant type, and patient health risk factors [14][16][17]. These causes of instability and loosening are not independent from each other and the onset of any one cause may lead to the development or worsening of a related cause. By understanding the variation of extensor mechanism features and their effect on joint load and kinematics it may inform better implant designs and surgical decisions leading to higher success rates of surgical intervention.

2.1. Patella Thickness

Patella thickness has been attributed to a range of complications following TKA, including anterior knee pain, patella component failure, patella fracture, decreased flexion range, and subluxation [18][19][20][21]. The benefit of resecting the patella is still disputed. Some studies claim that patients with non-resurfaced patella are more likely to develop anterior knee pain that will later require revision surgery to resurface the patella [22][23]. While other studies claim that revision does not significantly reduce rates of anterior knee pain and introduces the potential for catastrophic failure of the component [24]. This controversy is highlighted by the variability in patellar resurfacing rates around the world, ranging from 2% - 90% of cases [25]. Despite this variability and controversy, significant deviation from natural patella thickness may occur after patella resurfacing performed during a TKA.

When resurfacing patella, the goal of the surgeon is either to restore the patella to the native thickness [24][26][27][28], or to limit patella joint complex thickness to a predetermined maximum,

typically 25mm in men and 23mm in women [25]. When this is not possible and the final thickness of the patella is greater than the natural thickness, it is referred to as 'overstuffing' of the PF joint.

Surgeons are also typically advised to maintain a post-resection bony patellar thickness of at least 15mm to avoid excessive patella strain that may increase fracture risk [29]. However, surgeons only have a limited set of patella component sizes to choose from, since companies produce components at a thickness between 7-10mm. Resurfacing a patella under these constraints is not always possible, particularly in patients with deteriorated or naturally thin patellae [26]. In order to restore natural patella thickness in patients with thin patella, the resected bony thickness may need to be as low as 9mm (patella have been reported as thin as 18mm) [26][27][28]. The resulting variation in thickness leads to differences in strain, contact force/pressure, and kinematics.

Kinematics and Kinetics

The patella anterior bone strain has been shown to increase as the residual thickness decreases [28][29][30]. This is related to differences in peak quadriceps force and the amount of bone available to distribute the load. In a thin patella the peak quadriceps force is higher at low flexion angles ($< 40^\circ$) and lower at higher flexion ($> 80^\circ$) [28]. This change in quadriceps load related to patella thickness is supported by the observed mechanical advantage as well, showing that thick patella reduce quadriceps force and thin patella increase quadriceps force during extension [31][32]. Patella thickness changes the resulting moment arm of the quadriceps muscle which results in either increasing or decreasing the strain on the patella [2]. Significant increases in bone strain have been reported for patella with residual bone thickness less than 13mm - 15mm [28][29].

These higher strains are associated with increased risk of anterior knee pain and patella fracture, particularly for patients with pre-existing conditions such as rheumatoid arthritis and inflammation [25][28][33]. While these findings support the recommendation to maintain a thickness of at least

15mm, good clinical results have also been documented for resected thickness less than 12mm in patients with naturally small patellae [26].

Anterior-posterior (AP) forces and superior-inferior (SI) shear forces acting on the patella have been found to increase as total resurfaced patella thickness increases [34][35]. This effect may be more detrimental due to the geometry of the resurfaced patellar component. Resurfaced patellae are less conforming than the natural geometry. The component contact area has been reported as low as 21% of the contact area in the natural knee (depending on component design) [36]. The combined effect of increased forces acting on thicker patella, with decreased contact area due to poorly conforming geometries (reducing the bearing surface), indicates an increase in both equivalent stress on the patella and risk of component failure.

Patella thickness also has a significant effect on overall joint kinematics. In native knee structures the patella will tilt medially from 0°-15° flexion and then proceed to tilt laterally beyond 15° flexion [28][37][38]. Variations in patella thickness generally affect the lateral tilt and total range of flexion of the knee. Increases in patella thickness results in greater lateral tilt throughout the range of flexion [18][28][38]. The effect of thickness on flexion range is unclear. Some studies have reported no significant change to range of flexion while several intraoperative studies report significant changes in passive knee flexion for increases in patella thickness greater than 6mm. These studies have reported decreases in flexion range on the order of 1.2° - 3° per 2mm increase in patella thickness [18][39][40]. As patella thickness increases the patellar contact location changes [28], resulting in increased lateral shift in early knee flexion and medial patellar shift in late flexion, at angles greater than 45 degrees, compared to the natural knee [18][37][38].

The majority of research related to patella thickness focuses on changes in patellar loads or patellofemoral kinematics; however, effects have been reported to tibiofemoral kinematics as well. The primary effect on TF motion is increased tibial internal rotation at flexion angles greater than 50°. This

change is accompanied by an increased posterior shift of the medial femoral condyle [41]. This could be partially attributed to reported increases in medial shift of the patella as the thickness increases. A medial shift increases the Q-angle (from the coronal plane, often defined as the angle between the quadriceps load vector and patellar ligament load vector) and changes the line of action at the tibia which effects tibia rotation relative to the femur [37].

Surgical Techniques

During patellar resection and resurfacing the surgeon must be aware of resection symmetry, resection depth, and restoration thickness [42]. Resection technique may have a large impact on all of these factors that may ultimately determine the necessity of additional intraoperative soft tissue balancing and postoperative success. Patella resection is most commonly performed with a cutting guide; however, other techniques have been developed such as a freehand haptic feedback method and a four quadrant resection method [42][43]. The aim is to reduce the amount of variability in patellar resection. These alternate methods have significantly increased the accuracy of achieving desired patella thickness and symmetry [42].

Once the patella has been resurfaced, the surgeon will manually articulate the joint to ensure proper patella tracking and joint balance. A typical patella tracking error is increased lateral tilt during passive flexion. Typical causes of lateral tilt are related to patellar component medialization, improper patellar resection angle (thinning of the medial patella), patella overstuffing, and internal rotation or medialization of the femoral component [36][44][45]. To avoid abnormal lateral tilt, the surgeon must pay close attention to the bone cuts and placement of these components. In the presence of abnormal lateral tilt, a common procedure to correct this abnormal motion is a lateral retinacular release of the medial patellofemoral ligament (MPFL) [38][46]. While this is a common procedure to reduce lateral tilt, it may have added effects of pronounced medial tilt and abnormal tibia external rotation. The increased tibia rotation could be explained by the increased effect from the iliotibial band after the release [38].

Surgeons must also be aware of soft tissue structures surrounding the patellofemoral joint. The combination of medial incision, lateral release, and removal of the patellar fat pad may affect the patellar blood supply, potentially leading to avascular necrosis and patellar fracture or component loosening [47]. The motion of the quadriceps tendon along the femur in deep flexion can degrade the tissue resulting in a condition referred to as patellar clunk. This can occur due to superior overhang of the patellar component or femoral component design (typically cam mechanism of posterior stabilized components) [36][47].

2.2.Joint Line Elevation

Methods to define patellar height have been in practice since the 1930's. The earliest, commonly used practical method to assess patellar height was developed in 1938 using radiographic techniques [48][49]. Since then, many other techniques have been developed in an effort to improve measurement reproducibility and accuracy, and to account for limitations of existing methods [48]. In general, there are two primary methods of determining patellar height: indirect or direct. The indirect method describes measurements that relate the position of the patella to the tibia and the direct method relates the position of the patella to the femur [48]. The most commonly used measurement methods are indirect. Four indirect methods that are typically used include the Insall-Salvati ratio, Modified Insall-Salvati ratio, Balckburne and Peel index, and the Caton Deschamps index. These are popular methods as they tend to be easy to use and are applicable over a wide range of flexion angles, when applied to radiographs. Direct measurements rely on distal femoral locations to define patella height, and are typically only applicable at specific flexion angles due to femoral rollback. These methods are difficult to use and as a result are referenced less frequently [48][49].

Despite the frequent use of the four common indirect measurement methods, there are still concerns over their accuracy. The calculated patella height varies significantly based on patient position

and quadriceps muscle activation at the time the image is taken [49]. Attempts to account for patient position variability continue to result in new methods to determine patella height, such as the “knee triangular ratio” [49]. This continued development of measurement methods and varied use indicates that an agreed upon definition of patella height has yet to be achieved. Different measurement methods may result in differences in how knees are classified and affect the conclusions of a study accordingly.

There are two definitions for abnormal patella height, patella alta (or patella superior), and patella baja (or patella inferi). These positions are typically identified by a threshold defined by the particular measurement method being used [48]. Patella baja is also frequently referred to as pseudo patella baja in the case of joint line elevation, patellar tendon adhesion or distal tibial osteotomy [50][51][52][53]. Pseudo patella baja is identified when the patella appears to have moved distally in reference to the femur or joint line, not as a result of changing patellar tendon length, which can be caused by trauma or direct surgical manipulation of the ligament. Pseudo patella baja is typically a result from TKA due to poor bone cuts or improperly sized components. In the case of this review, no distinction between patella baja and pseudo patella baja will be made, unless otherwise specified, as they are effectively the same.

Kinematics and Kinetics

There are different biomechanical effects depending on the position of the joint line relative to the patella height. In typical patellofemoral mechanics, peak patellar compressive load occurs at 80° knee flexion and then decreases due to increased load sharing from the quadriceps tendon wrapping. The load distribution on the posterior face of the patella typically moves from a distal position at extension to a proximal position at deep flexion [3][36]. The patella shifts medially in early flexion until

it engages the trochlear groove near 20° flexion along the lateral face of the patella. It then starts to move laterally with increasing lateral tilt [11][54].

Studies related to biomechanical effects from patella alta are scarce and the overall effects are poorly understood. Most literature focuses on surgical procedures intended to address persistent mechanical deficiencies related to patella alta. Patella alta position is likely to result in increased lateral patella shift and tilt in early flexion (< 20°) [55]. Patella alta is also associated with an increased rate of patella dislocations [56]. These problems arise in part due to the patella not being engaged in the trochlear groove until later in flexion compared to a knee with a neutral patellar position [54][55]. Patella alta occurring from the malposition of TKA components and joint line distalization results in increased observed joint stiffness. This also shows reduced changes in tibial rotation and posterior displacement of the femoral condyles during flexion [57].

Several kinematic effects due to joint line elevation and patella baja have been observed after TKA. In knees with an elevated joint line the femur tended to translate posteriorly at full extension. In cruciate retaining implants, increased joint line significantly strained the PCL beyond 60° flexion, requiring PCL release to avoid the femur from dislocating posteriorly [57][58][59]. In cruciate retaining designs, the associated decrease in quadriceps load and PF contact force after joint line elevation have been attributed to increased PCL strain and a resistance to flexion rather than an improved moment arm [59]. Tibia rotation was unaffected and may be due to the symmetric nature of the implants [57][58]. Mid-flexion laxity increase (stiffness decrease) has been observed with an elevated joint line that may lead to later instability [57][60]. A significant increase in PF flexion has been observed as joint elevation increases [61].

In cases where patella baja occurs due to shortened patella ligaments the PF flexion angle increases with insignificant changes in TF function [53][62]. These results are similar to those observed in joint line elevation due to TKA.

Despite the stated importance of restoring natural joint line and its implied effect on TKA failure, the kinematic changes due to changes in patella height and joint line are poorly understood. Reported changes focus on decreased range of TF flexion, increased PF flexion angles, poor clinical scores and increased pain. More focus seems to have been paid to the effect on joint loads, which may have a larger impact on component failure. Unexpectedly joint loads could contribute to instability or component loosening and failure.

In cases of patella alta (joint line distalization) a mechanical advantage exists between 0° - 60° flexion as the moment arm is extended. This implies lower required quadriceps force for required motions within this range [63]. This improved efficiency in turn results in lower PF contact forces in this range [64]. A joint line distalization of 5mm has a predicted decrease of PF joint force up to 11% body weight during walking and 30% body weight during stair ascent [65]. Despite the reduced AP load at the PF joint, it has been observed that the lateral PF joint load increases, which may explain the tendency for dislocation of patella alta patients [66]. This mechanical advantage of patella alta is reversed at flexion angles beyond 60° . At these higher flexion angles the peak joint force increases significantly with increased patella height. This is in part due to delayed onset of quadriceps tendon wrapping that is supposed to contribute to load distribution and decreased mechanical advantage in this position [63][64]. The opposite effect is true in cases of patella baja or joint line elevation, with significant increases in PF joint force in early to mid-flexion [65][67]. The relationship between joint contact area and joint stress is less clear. Reduced contact area has been observed in both cases of patella alta and elevated joint line. In cases of elevated joint line the decreased contact area was observed at late (high) flexion angles [61], and in patella alta decreased contact area was observed in early (low) flexion [55]. PF and TF contact stress in joint line elevation was largely unchanged and only noticed a difference at extreme joint line changes [58][61]. In the case of an in vivo study, the contact stress was not seen to change in the presence of patella alta, however this was attributed to compensatory strategies imparted

by the subjects to avoid increasing stress and possible anterior knee pain [68]. Changes in TF loads are poorly understood due to patella height, however studies that have investigated compressive TF loads report little to no effect [58][65].

Surgical Techniques

A deviation in tibiofemoral joint line is a well-documented phenomenon after TKA. Changes in height have been a suspected source of mid-flexion instability, pain, patellar impingement, component failure, and attributed to compromised biomechanical function [51][69][70][71][72][52][73][74]. A common guideline is to restore the joint line to within 5-mm after TKA as good clinical outcomes and mechanical performance have been observed within this limit [75].

Joint line proximalization after TKA occurs from excessive distal femoral bone loss. When excessive bone loss occurs the femoral component sits more proximally on the femur requiring a thicker tibia insert which effectively raises the joint line. This bone loss can be caused by primary surgical bone cuts from using an undersized femoral component, or minimal resection of the tibial plateau, or distal femoral bone loss during revision surgery after removal of the primary femoral component [70][74][76][50][75]. An undersized femoral component requires that more femoral bone be removed to get a proper fit of the component. Minimal tibia resection may result in inadequate gap space for the inserts, leading to greater distal femoral resection to create the necessary space. Joint line shift from distal femoral bone loss is more common after revision TKA rather than primary TKA due to good bony fusion to the femoral component, or compromised bone from stress shielding or osteolysis [70][71][76][72].

To correct pseudo patella baja due to excessive distal femoral bone resection, the femoral component must be adjusted and/or replaced [50]. Adjustments to the femoral component are done using distal femoral augments to reposition the component distally. This method is able to account for

excessive bone loss and reduce the joint gap to avoid using a thick tibia insert that would otherwise raise the joint line. In one study, the use of augments resulted in the restoration of joint line to within 5mm in 63% of cases [77]. The study found that when the joint line was not restored to within 5mm the clinical knee society score was much lower [77][72][74]. Patella alta resulting from joint line distalization after TKA is less common but may result if the patella position is not lowered during primary TKA or if a patellar tendon release is performed and the patella moves too far proximally [75].

True patella baja due to changes in patellar ligament can occur post-surgery for several reasons. The presence of scar tissue, shrinking of the patellar ligament (infrapatellar contracture syndrome), or patellar ligament fusion to the tibia effectively shortens the patellar ligament and results in lowering the patella [50][53][74]. True patella alta is typically caused by a long patella ligament rather than a distal tubercle attachment site [78][79].

There are two types of surgical intervention that can restore normal patella height, changing the length of the patellar ligament or tibia tuberosity osteotomy. Lengthening of the patellar ligament is performed to correct for patella baja and can be achieved either through ligament release or through a z-plasty technique [80][50][54][75]. Shortening the patellar ligament is done to correct for patella alta. This can be done using a horizontal mattress suture method, where the ligament is folded over itself and sutured together [54]. Tibia tuberosity osteotomy effectively moves the insertion site of the patellar ligament. Moving the attachment site distal and posterior will move the patella distal, and vice versa [81][82]. These procedures are typically performed in the absence of TKA to improve natural stability and function. Any variation in patella height has a direct effect on biomechanical function and is a primary factor prior to any surgical procedure.

2.3. Tibia Tuberosity Location

The tibia tuberosity is a bony protrusion located anterior and slightly distal to the tibial plateau. This is the insertion location of the patellar ligament and is a part of the quadriceps extensor mechanism. The literature regarding the position of this insertion point and its effect on kinematics is limited. Most studies focus on tuberosity osteotomies that aim to alter the insertion point of the patellar ligament and their relative clinical success to alter PF maltracking and instability.

Kinematic and Kinetics

Due to the fixed length of the patellar tendon, whenever an osteotomy is performed the patella position will be changed, which is the primary purpose of the procedure. For this same reason it is not possible to isolate the effect of tuberosity position independent of patella position, aside of computational modeling. As such, most effort has gone into understanding changes in PF and TF function as it relates to clinical success [83][84][85][78]. In vitro testing also presents many difficulties and requires creating a malalignment condition in order to study the effect of a repositioned tuberosity [8]. These limitations are partly responsible for the limited data on the effect of tuberosity position on total joint kinematics.

Medialization/Lateralization:

Studies showing the effect of medialization and anteromedialization on a mal-aligned knee are scarce and Kinematic changes of the PF joint after medialization of the tuberosity position resulted in reduced lateral patellar tilt and shift near full extension, between 0°-20° [6][8]. There is no significant reported change in patellar rotation (about the AP axis). Anteromedialization was shown to increase lateral patellar tilt over all flexion angles, differing from the trend seen in pure medialization [8].

Medialization caused a significant increase in external tibia rotation, especially near 40° flexion. The increase in external rotation is approximately 2° - 13° [6][7]. This wide range of reported external rotation may be due to the difference in accounting for soft tissue constraint between studies. When

hamstring activation is added, the tibia is rotated slightly internally, reducing the magnitude of external rotational changes [7]. After medialization significant increases in lateral and posterior shift of the tibia were observed at 40° flexion [6][7]. Anteromedialization showed similar trends to changes in TF kinematics as pure medialization, with a greater magnitude of tibia posterior shift [7].

Changes in PF kinematics lead to changes in contact area and pressure which is thought to be related to anterior knee pain, joint degeneration, and osteoarthritis [86][87][88][89]. Medialization of the tibia tubercle results in decreased mean and peak PF contact pressure and force. Due to decreased lateral patellar tilt the contact pressure in the lateral patellar facet is decreased and the pressure in the medial facet is increased [5][8][86][90]. Care must be made as extreme medial displacement can result in increased total PF contact pressure and force [88]. The magnitude of peak pressure decreases tend to be larger after implemented anteromedialization of the tibia tubercle, especially at lower flexion angles [5][8][9][87]. The data regarding PF contact area after medialization is less clear. Some studies have shown decreases in contact area and others have shown little to no change [8][82].

Medialization also plays a role in tibiofemoral contact pressures. After medialization, contact pressure in the medial condyle increased, while lateral contact force decreased and it was only significant after 15mm of medialization of the tuberosity [9][88]. Increases in PCL load after anteriorization of the tubercle have also been observed at large flexion angles and decreased in ACL load at low flexion angles [9].

Proximal / Distal Tuberosity Translation:

To the author's knowledge there have been no studies conducted to determine the kinematic and kinetic effects from a proximal or distal transfer of the tibia tuberosity, independent of change in patella height. This kind of procedure is typically performed to correct symptoms of patella alta and baja and most research consists of retrospective clinical assessments [78][85]. Further work needs to be done to

better understand the effect tuberosity SI distance has on biomechanical function. These results tend to be similar as those that look at altering patella ligament length to correct patella height.

Surgical Techniques

There are several different osteotomy procedures that exist depending on the type of desired change [82]. Each procedure may have many variations on osteotomy techniques leading to more than 100 different surgical procedures to treat PF instability [91]. The goal of a tuberosity osteotomy is to change medial-lateral position, anterior-posterior position, distal-proximal position, or some combination, to improve mechanical function.

Efforts to treat patellar instability started with medial transfer of the tubercle to correct patellar tracking by changing the line of action of the extensor mechanism. The earliest medialization technique was the Roux procedure which was later replaced with the popular Elsie and Trillat procedure. The latter has shown good clinical results and few poor outcomes following surgery, with success rates above 60% [81][82]. Long term follow up shows that this procedure may lead to increased rates of osteoarthritis due to changes in PF contact mechanics [82].

Maquet was the first to describe a procedure for pure anterior shift. The goal of this procedure is to reduce the force in the patellar tendon and therefore decrease patellofemoral contact pressure. This procedure was initially met with results that indicated a high success rate. After long term follow ups this procedure had a similar problem as the Hauser procedure, showing deterioration of results [82]. This procedure primarily fell out of favor due to the common complication of skin necrosis. The suggested cause was increased skin tension after anteriorization of the tubercle [82].

There are several procedures that have been developed that combine medialization and anterior-posterior shifts that attempt to further improve stability and function. The Hauser procedure was created to move the position both medial and posterior. This procedure was shown to have high

initial clinical success rates. However, this procedure has increased rates of anterior knee pain and onset of osteoarthritis at long term follow up [82]. Due to poor long term performance this procedure is not typically used. The Faulkerson procedure moves the tuberosity medial and anterior. The goal is to address mechanical alignment and total load on the PF joint. This is a popular method that has shown good results without the associated onset of osteoarthritis [82]

A procedure for distalization and proximalization of the tubercle was introduced by Caton in 1982 [81][82]. This procedure is typically done in order to correct patella alta (in cases of patellar instability) or patella baja (in cases of knee stiffness or pain). In distal osteotomy a success rate of 78% was reported and for proximal osteotomy a success rate of 83% was recorded [81]. Proximalization was only performed if the pathology was mechanical and it was determined to be directly related to tuberosity position and if the patella tendon was a satisfactory length (2.5mm is recommended by author) [81]. There is no data for long term follow up regarding this procedure [82].

Each of these procedures attempt to improve patellofemoral kinematics and stability, however each procedure has a similar risk of long term joint degeneration and onset of osteoarthritis. Small changes in tuberosity position can have a significant impact on patellofemoral joint kinematics and contact pressure. The prevalence of long term development of osteoarthritis suggests that the effects of tuberosity position on patellofemoral and tibiofemoral kinematics and pressures is still poorly understood.

Significant biomechanical effects have been observed due to variability in patella thickness, joint line elevation, and tibia tubercle position. These factors are directly linked to one another and due to the nature of the fixed parameters of the extensor mechanism it is rarely possible to change one factor without also changing at least one other. Changing these features often change either the patellar ligament angle or the Q-angle which alters the muscle line of action [92][93]. Changing these angles has been shown to affect the PF and TF kinematics as well as soft tissue loads. These effects must be

considered prior to any surgical intervention of the knee to ensure the appropriate adjustments are made to effectively improve overall knee function and stability.

3. Effect of Variability of Extensor Mechanism Features on kinematics and Tibiofemoral anteroposterior loads

3.1. Introduction and Background

The primary function of the extensor mechanism is to control flexion-extension of the tibia relative to the femur during quadriceps muscle contraction. This function is affected by morphology of the femur, tibia, and patella and by the soft tissue structures of the quadriceps tendons and patella ligament. The focus of this study is on the variability of three extensor mechanism features and their overall effect on joint kinematics and loads. The features being investigated are patella thickness, patella height from the joint line, and tibia tuberosity position relative to the center of the tibial plateau.

Changes in patella thickness after resurfacing from a TKA is often linked to patella fracture risk and changes in range of motion and PF stability [19][20][21][25]. As the amount of residual bony thickness decreases the patellar strain increases [2][28][30] [33][34][35]. This occurs as there is less bone to distribute the load applied by the quadriceps. This increased strain is a concern for fracture risk, so it is common for surgeons to maintain a minimum residual thickness of 15mm [29]. Increasing the thickness, or “overstuffing” of the joint has been attributed to decreased range of motion and increased risk of patella dislocation [24][47]. Overstuffing has been shown to increase lateral patella tilt and decrease overall range of motion by 1.2°-3° per 2mm increase in thickness [18][39][40]. This overstuffing can occur if the surgeon attempts to maintain the minimum residual thickness on patients with naturally thin patellae or if a femur component with greater anterior displacement is implanted [26].

Variation in patella height or movement of the joint line, either proximal or distal, after TKA can have adverse effects on patellar stability, pain, and range of motion [70][71][72][73][74][75]. Minimal changes to PF and TF kinematics have been observed due to changes in patella height. The majority of research looks at the effect of changing patella height on PF and TF contact pressure/force. Patella alta (or distalized joint line) have shown a decrease in total peak PF contact pressure and force at flexion angles $<60^\circ$ due to greater mechanical advantage. Greater peak PF contact pressure and force occur at deep flexion due to decreased mechanical advantage and late onset of quadriceps tendon wrapping at the femur [63][64][65]. The opposite trend in PF force is observed in cases of patella baja. Higher patellae also are at higher risk of dislocation due to increased patella tilt and late engagement of the trochlear groove [55]. Patella alta has also been shown to reduce peak TF contact force while patella baja (due to significant joint line elevation) has been shown to increase TF contact force at low flexion angles [65].

Effects of medial-lateral tuberosity position are typically investigated as a part of patellar instability. It is commonly measured as the TT-TG (tibia tuberosity – trochlear groove) width. A large TT-TG width is an indicator of patellar instability and an increased risk of patella dislocation [10]. By moving the tuberosity medially in patients with a large TT-TG width, the peak PF contact force and lateral tilt was decreased [5][6][8][87][90]. This also caused increased external TF rotation in mid-flexion [6][7]. However, changing this width too far or in patients with a normal width may cause increased peak PF contact force [88]. Anteriorization of the tubercle is primarily done to reduce PF force and has been shown to increase PCL strain at late flexion [9]. Changes in proximal/distal position are typically only done to alter patella height. The effects of this movement are less understood, consisting of mostly retrospective studies [78][85]. These effects reveal a significant relationship between the tubercle position and PF and TF kinematics.

The commonality between these three features is that changes to any of them will alter the patella tendon angle relative to the tibia long axis and, to a lesser extent, the Q-angle [92][93]. Changes in these angles result in changes in the quadriceps muscle line of action, and change the moment arm and associated mechanical advantage. The changing mechanical advantage alters the required quadriceps force to extend the tibia. It is also often not possible to change just a single one of these features. For example, if the patella thickness is changed then so is the height from the joint line. By increasing thickness the patella moves out, and due to the fixed length of the patella tendon it will also move proximal to the joint line.

A common method to study knee kinematics and kinetics is in vitro testing, often using oxford style, dynamic motion simulators [94][95][96][97]. Typically the selected simulations aim to replicate daily living activities that patients will commonly perform after surgery, including walking, stair ascent/descent, squats, and pivoting maneuvers. The simulator used for this study is the Kansas Knee Simulator (KKS). This simulator aims to replicate both tibiofemoral (TF) joint loads and flexion angle of a specific activity. Target joint load and flexion come from published data recorded in vivo [98] or through wear simulation standards [ISO 14243-1, 2002]. These targets are achieved in the KKS through the control of five linear hydraulic actuators. In order to determine the required motion of each actuator, the simulator is operated with analog prosthetic components prior to using cadaver tissue [99]. Previous work done to determine actuator targets [100] using the existing analog prosthetic configuration results in discrepancies of TF anterior/posterior (AP) joint loads when applied to cadaver specimens. To properly control the AP load at the TF joint using analog components, sagittal-plane features of the extensor mechanism must be set in the simulator to properly represent a physiologic condition.

The first goal of this study is to determine a desired configuration for patella thickness, patella height, and tuberosity position, using analog components in an oxford style knee simulator that will

more closely match in vitro measured tibiofemoral AP joint loads. Second, determine how natural variations of the three extensor mechanism features relate to kinematic variations. By understanding how these features relate to joint loads and kinematic performance steps can be taken to improve TKA design, inform surgical decisions, and reduce long term TKA failure rates and improve overall outcomes.

Significant changes to these three features have been attributed to failure of total knee arthroplasty (TKA) components. The most common reason for TKA failure is aseptic loosening of the components, followed by infection, wear, and instability [13][14][15]. The underlying causes behind these failure rates are poorly understood and have been attributed to different factors, including poor gap balancing, component malpositioning, ligament/tendon insufficiency, muscle insufficiency, extensor mechanism insufficiency, and patient health risk factors [14][16][17]. These factors are often interrelated and one factor may introduce, or worsen, any other factor, ultimately leading to component failure or revision. Understanding the role of the extensor mechanism on joint loads and kinematics may reduce the amount of component failures after TKA.

3.2. Materials and Methods

All tests conducted in this study were done using the Kansas Knee Simulator (KKS). The KKS is an Oxford style dynamic knee simulator with five hydraulic axes of control [100][101]. The axes under control are the hip flexion, vertical load, ankle load, medial/lateral load, and internal/external torque applied about the long axis of the tibia. These axes are each controlled such that specific joint loads at the knee can be simulated for different activities. For this study, the KKS controlled hip flexion angle (a function of knee angle) by pulling on the quadriceps tendon, and joint loads were simulated by controlling the load at each of the remaining four actuators. The simulated motions typically targeted joint loads seen in daily living activities (i.e. walking, stair ascent, squatting). Compressive tibiofemoral (TF) loads were achieved by specifying a vertical actuator load and ankle flexion moment. The resulting

quadriceps force was allowed to vary to achieve a targeted flexion angle, Figure 1. The function of the three sagittal plane actuators are all interrelated. For example, increased ankle flexion moment will drive the knee to extend, requiring a decreased quadriceps load to maintain a given flexion angle, and a decreased vertical load to maintain compression.

TF joint loads were measured in this study using a custom made, implantable, instrumented tibia tray (ITT) developed by DePuy Synthes (DePuy Synthes, Warsaw, IN, USA). This tibia tray was designed to be used with a size 8, primary Attune total knee replacement. The ITT is split into three compartments (medial, lateral, and central) each containing a six-degree-of-freedom (DOF) piezoelectric load cell, Figure 2. Total loads were determined based on the sum of the loads from each compartment. ITT data were collected at a frequency of 100 Hz using a custom LabView program, and KKS sensor data were collected at 1kHz in LabView. All data were filtered using a low-pass fourth-order butterworth filter.

This study analyzed two dynamic motion profiles, a simple squat (SS) and a walk. The simple squat profile controls the hip flexion and ankle load actuators in the form of sine waves. The input profile for each actuator was a sine wave with a period of 20 seconds, with peak hip angle and peak ankle load at the mid-point of the cycle, Figure 3. A positive ankle load applies a posterior directed force on the tibia, forcing the tibia into the femur, creating compressive TF loads and reducing quadriceps load at high flexion angles. The peak TF flexion angle of the squat profile is 110° , which is double that of the measured hip angle. This assumes that the tibia and femur are exactly the same length from the TF-FE axis of rotation.

There are two different walk profiles that were used in this study. The first walk profile ("WalkDOE") was used to analyze TF joint loads. This profile is based on work by Bergman [98] that has measured total TF joint loads for all six DOF at the knee using a specially designed instrumented tibia tray (ITT). The reported flexion-extension angle and modified superior/inferior (SI) and

anterior/posterior (AP) loads for the average walk were used as input profiles for the KKS actuators (to ensure constant compression and stability in the KKS). A previously developed neural network method was used to generate the actuator profiles on the KKS to simulate the desired input targets [100], Figure 3. This walk profile was created using two cadaveric knees, one knee was used as training data for the neural network and the other knee was used as verification. This verification knee represents the baseline performance as the desired target for joint loads (“Cadaver Target”).

The second walk profile (“WalkCAD”) was used for kinematic evaluation of cadaver data and is based on published standardized joint loads [ISO 14243-1, 2002]. The knee flexion angle, AP load and SI load from this standard were used as inputs to a multibody dynamic model of the KKS created using Adams [MSC Software Co. Newport Beach, CA, USA]. A MatLab/Simulink model of the PID control system of the KKS was run in conjunction with the Adams model to calculate the required actuator profiles to achieve the desired inputs [99][102]. This method resulted in different actuator targets, and thus a different walk profile compared to WalkDOE, Figure 3.

Kinematic data were collected using an active Optotrak motion capture system (Northern Digital Inc., Waterloo, Ontario, Canada)[103]. Rigid bodies with infrared light emitting diodes (IREDs) were fixed to the femur, tibia, and patella. Data were collected at a frequency of 100 Hz. Tibiofemoral kinematics are described using the Grood-Suntay (GS), three-cylindrical, open-chain coordinate system and patellofemoral kinematics use a modified GS description. PF kinematics use define all rotations based on the GS coordinate system with all three translations along a fixed femoral coordinate system [104][105], Figure 4.

3.2.1. Tibiofemoral AP Load Evaluation

A design of experiments (DOE) was established to analyze the sensitivity of the three factors thought to affect total tibiofemoral AP joint load. The three factors being analyzed are patella height from the

joint line, patella thickness, and tibia tuberosity position. Each of the factors was varied between three levels within a normal anatomical distribution (Table 1). The Taguchi method was used to analyze this design of experiments, which resulted in an $L_9(3^3)$ orthogonal array of nine experiments. The nine experiments were all run in random order in three separate trials. All experiments were performed using analog fixtures of the total knee replacement components (components rigidly attached to aluminum fixtures in the KKS), including the ITT to measure joint loads. This removes any soft tissue effect and isolates the factors under study. The total knee replacement system used for testing was a size 8 Primary Attune total knee replacement developed by DePuy Synthes. The tibia insert was custom made to fit into the ITT and to isolate measured loads on the medial and lateral condyle and central post, Figure 2.

Mean reported patella thickness has been measured during total knee arthroplasty both before and after resurfacing. Average natural thickness has been reported as 22.6 mm with a range from 18 mm) to 30 mm, not accounting for gender or ethnic variances [27]. Tibia tuberosity positions were determined based on internal data provided by DePuy Synthes. A custom fixture was designed to vary the attachment between each position, Figure 5. Patella height was measured as SI distance between fixed body origins of the patella and tibia at a TF angle of 28°. The height measurements were taken from data collected from simulations performed in the KKS. This ensured that the quadriceps was loaded, thus providing a more accurate assessment of patella height.

Table 1: DOE Factors and the settings of all three levels for each.

Factor	Level 1	Level 2	Level 3
Patella Thickness (mm)	20.3	24.3	28.3
Patella Height (Joint Line Elevation) (mm)	26.6	35.5	44.4
Tibia Tuberosity Size [AP(mm)/SI(mm)]	5 [40.6/-29.3]	6 [44.5/-33.9]	7 [46.8/-40.2]

For each experimental set up the SS and WalkDOE profiles were simulated for a total of three cycles. The second cycle of each profile was isolated and used for data analysis. The data used for analysis were total measured AP load (sum of the medial, lateral, and central AP loads measured on the ITT). The error of total AP load was calculated by subtracting the Cadaver Target from the experimental trial AP load over the entire profile. A normalized RMS error value was calculated from the total error value for each experiment and then divided by the range of the Cadaver Target AP load. In this situation, quality loss is minimized by minimizing the normalized RMS error. The signal-to-noise (SN) ratio was calculated based on minimizing the normalized RMS error. The SN values for each experiment and each trial were averaged. The values were then reported for each factor and level to determine the desired levels that minimize the normalized RMS error in AP load. The sensitivity was calculated based on a sum of squares determined from the average SN values for each level of each factor.

3.2.2. Kinematic Evaluation

Natural knee kinematics were evaluated with 18 fresh frozen cadavers, reported as mean \pm one standard deviation (age 59.3 ± 13.2 years old, 25.1 ± 6.4 BMI, $69.7 \text{ in} \pm 2.6$ in height, ten right and eight left knees). Experiments were conducted between July, 2010 and January, 2015. Each specimen was thawed for 24 hours at room temperature prior to being dissected. The tibia was sectioned approximately 18 cm distal from the epicondylar axis. The femur was sectioned 28 cm proximal from the epicondylar axis. All soft tissue within 10 cm proximal and distal of the epicondylar axis was retained to maintain joint integrity. The remaining portions of the femur and tibia had all tissue removed and were cleaned and cemented with dental cement into cylindrical aluminum fixtures. Fixtures were aligned to be parallel to the intramedullary canals of the tibia and femur. The fibula was secured to the outside of the tibia fixture with a metal hose clamp to keep from moving during testing. Care was taken not to damage the heads of the quadriceps tendons so they could be cleaned and separated. Two

strips of sandpaper were superglued to the anterior and posterior surfaces of the rectus femoris and vastus intermedius quadriceps tendons and clamped into an aluminum fixture that can be attached to the quadriceps actuator in the KKS.

Each knee was secured in the KKS to simulate the dynamic walking motion. Prior to running any simulation the knee was cycled through a sinusoidal flexion-extension motion to make slight alterations to ensure that the leg was properly aligned (minimizing varus/valgus motion). Once the leg was set, the dynamic motion profile being simulated was run for 3-5 complete cycles. The middle cycle (second or third) was then isolated from the collected data and used for analysis. All 18 knees were evaluated with the WalkCAD profile.

A computerized tomography (CT) scan was taken of each leg prior to dissection. Solid models of the tibia and patella were obtained from these CT scans using 3D Slicer, open source segmentation software (v4.3.1, <http://www.slicer.org>). The solid models were imported into Altair, Hypermesh (v.13.0, Troy, MI, USA) and meshed using 1 mm triangle elements. The re-meshed models were used to determine the coordinates of selected anatomic features to get natural measurements of patella thickness and tuberosity position (both AP and SI distance). For consistent anatomic measurements the nodes of each solid model were rotated into a fixed body coordinate system.

The patella thickness was calculated as the absolute value of the AP distance between the most anterior and most posterior point of the patella. The tuberosity point was defined as the most anterior point of the tubercle. The SI and AP distance was calculated from the center of the tibial plateau, defined as the selected intercondylar notch (midpoint of the intercondylar eminences). Patella height was measured as SI distance between fixed body origins of the patella and tibia from simple squat profile simulated in the KKS. The height was taken at a calculated TF flexion angle of 22°, as this is the lowest common flexion angle between all trials.

Natural knee kinematics were analyzed using principal components to find correlations between changes in kinematic motion and quadriceps load to changes in the same three anatomic features investigated in the DOE. The data set included 18 observations (N=18), with the kinematic results of the simulated WalkCAD profile, which correspond to an individual knee. Kinematic and quadriceps load data points from the profile were taken at every 5% of the cycle, including the initial value (a total of 21 data points per profile, per kinematic motion). Both the quadriceps load and kinematic data were offset from the initial value to look at changes in load and motion. The TF kinematic motions included in the analysis are IE rotation, and AP translation, and the PF kinematic motions included are FE, IE (tilt), VV (spin), and ML. The number of kinematic variables included in the PC analysis is 126, and the number of quadriceps load data points is 21. Combining all of the variables with the anatomic measurements creates a PC data set with 151 variables (n=151).

Due to the different units and magnitudes of the measured variables, the input data were normalized to create a correlation matrix of size 18x151 (number of knees x number of variables). The eigenvectors and the eigenvalues of the correlation matrix describe the PC coefficients (loadings) and variances (latent values) respectively. Subsequent PCs were included for analysis until 80% of the total explained variation was met. This ensures that sufficient information from the original data is retained for analysis. The number of PCs used to represent the data was deemed sufficient once 80% of the total explained variation is met.

Each PC included in the analysis disturbs the corresponding PC by ± 3 standard deviations, while holding all other PC scores at the mean, and calculates a new value for each of the original variables. The perturbed plots are used to visualize the variability explained by the PC (i.e. what variables correlate to that PC and account for that variation in the data). The corresponding coefficients for each variable are plotted and color coded to help visualize the correlation between variables in each PC.

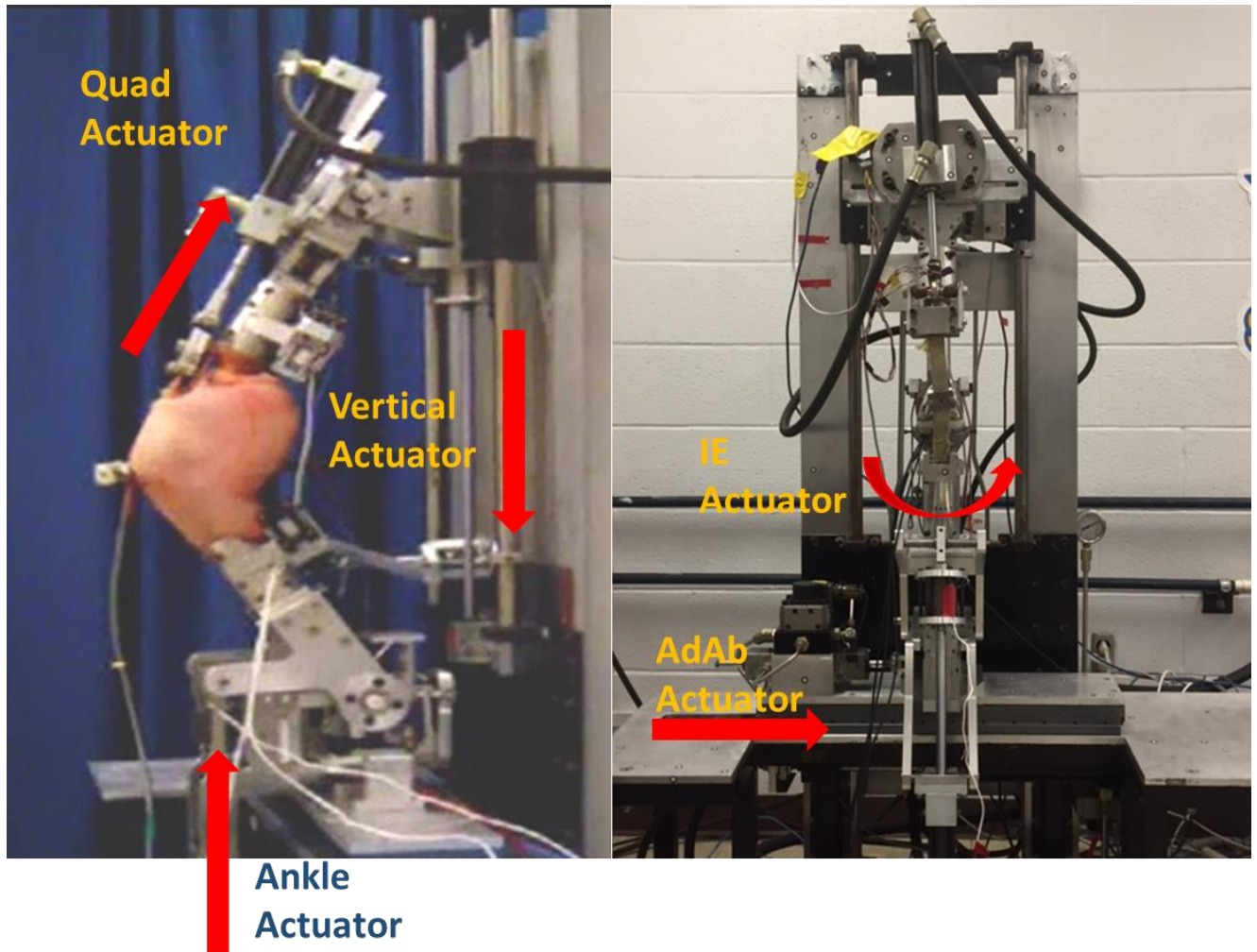


Figure 1: (Left) - Kansas Knee Simulator (KKS) with cadaver specimen under dynamic simulation. This figure shows the sagittal plane actuators (vertical load, ankle flexion moment, and quadriceps hip flexion). Motion from each actuator affects the others and influence flexion. The quadriceps load is free to change and is a result of the applied ankle and vertical actuator loads to achieve targeted flexion. (Right) – Shows the analog configuration and out of sagittal plane actuators (Internal-External torque and Adduction-Abduction moment).

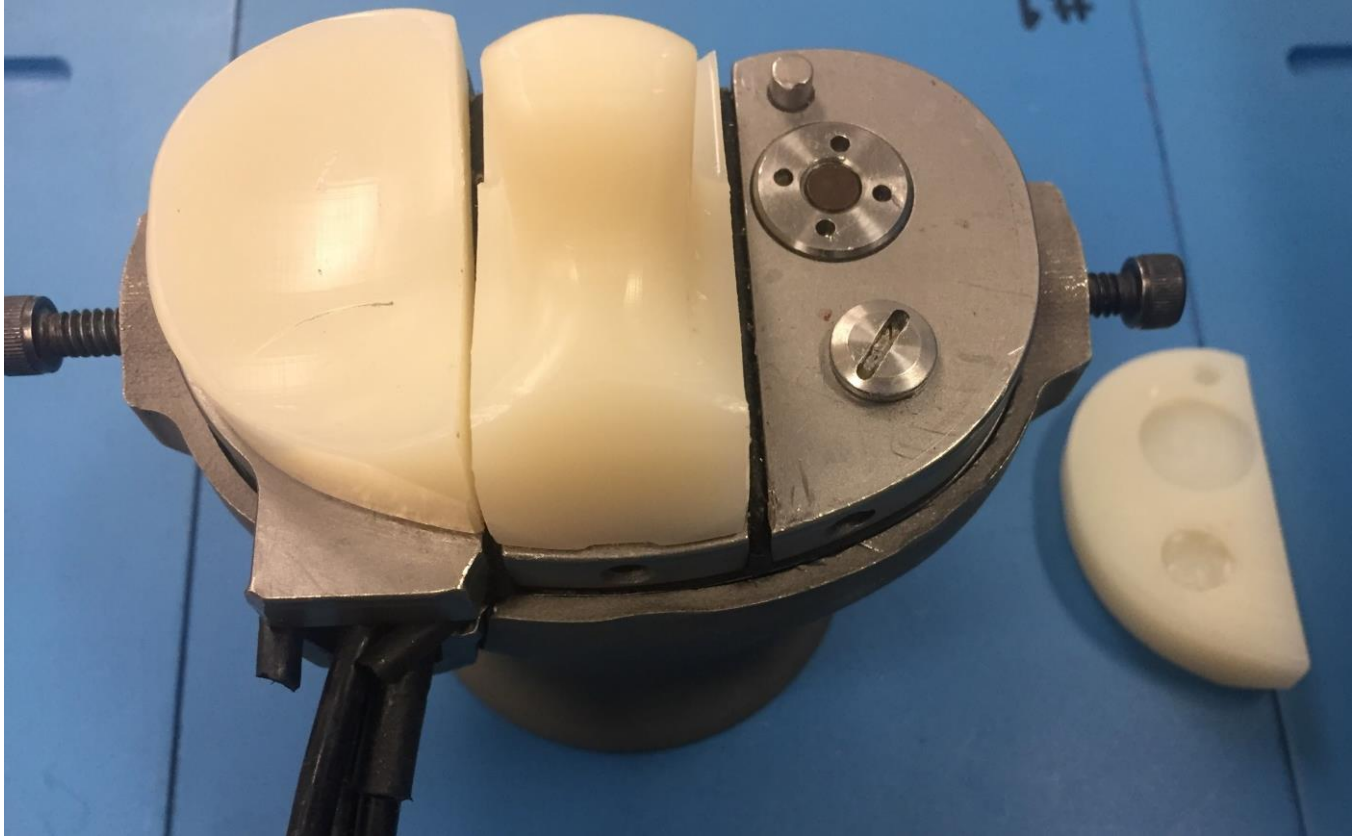


Figure 2: ITT Sensor used in DOE trials, with the lateral tibia insert removed to reveal the underlying lateral load cell. The insert shown is a DePuy Attune Primary implant, size 8.

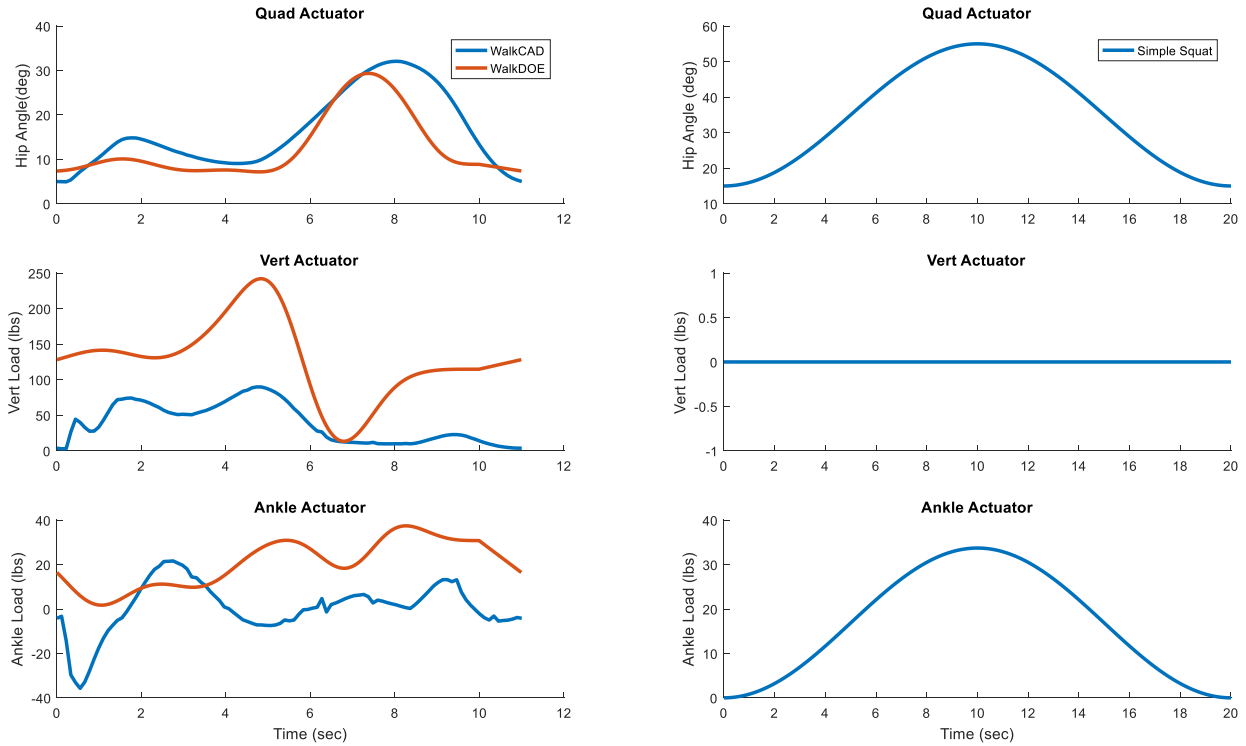


Figure 3: Dynamic simulation input profiles for KKS sagittal plan actuators. Plots on the left show actuator targets for walk profiles WalkCAD (used to evaluate natural knee kinematics) and WalkDOE (used to evaluate TF-AP loads). Plots on the right show the Simple Squat input profile actuator targets that were also used to evaluate TF-AP loads. Target loads are in pounds. Hip angle target is assuming that it is half of the TF flexion angle, so peak angle shown in the quadriceps actuator for the squat at 55° would correspond to a TF flexion angle of 110° at peak flexion. This assumes that the tibia and femur are identical lengths from the FE axis of rotation.

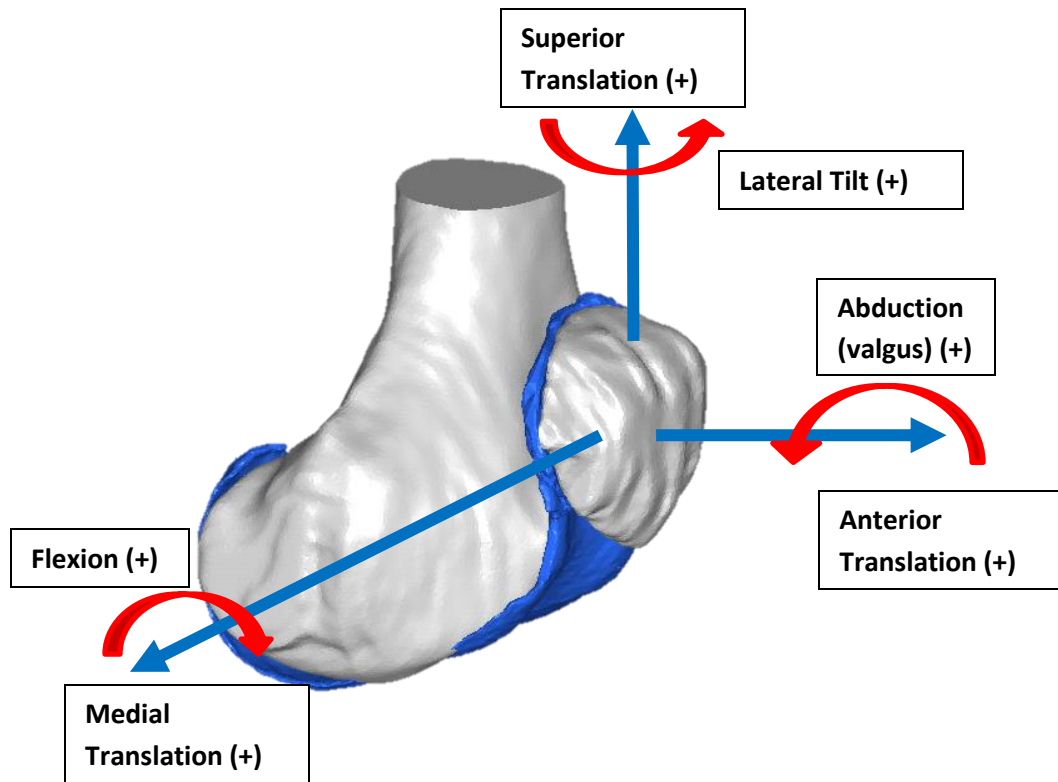


Figure 4: Groot-Suntay PF coordinates system and directions, as represented on a left knee. The same directions are applied to tibiofemoral kinematic descriptions, with the SI axis along the long axis of the tibia. The floating axis represents the AP axis, and SI movement is described as displacement from the femoral origin along the fixed body SI axis of the tibia/patella, and ML movement is along the flexion axis along the epicondylar width of the femur.

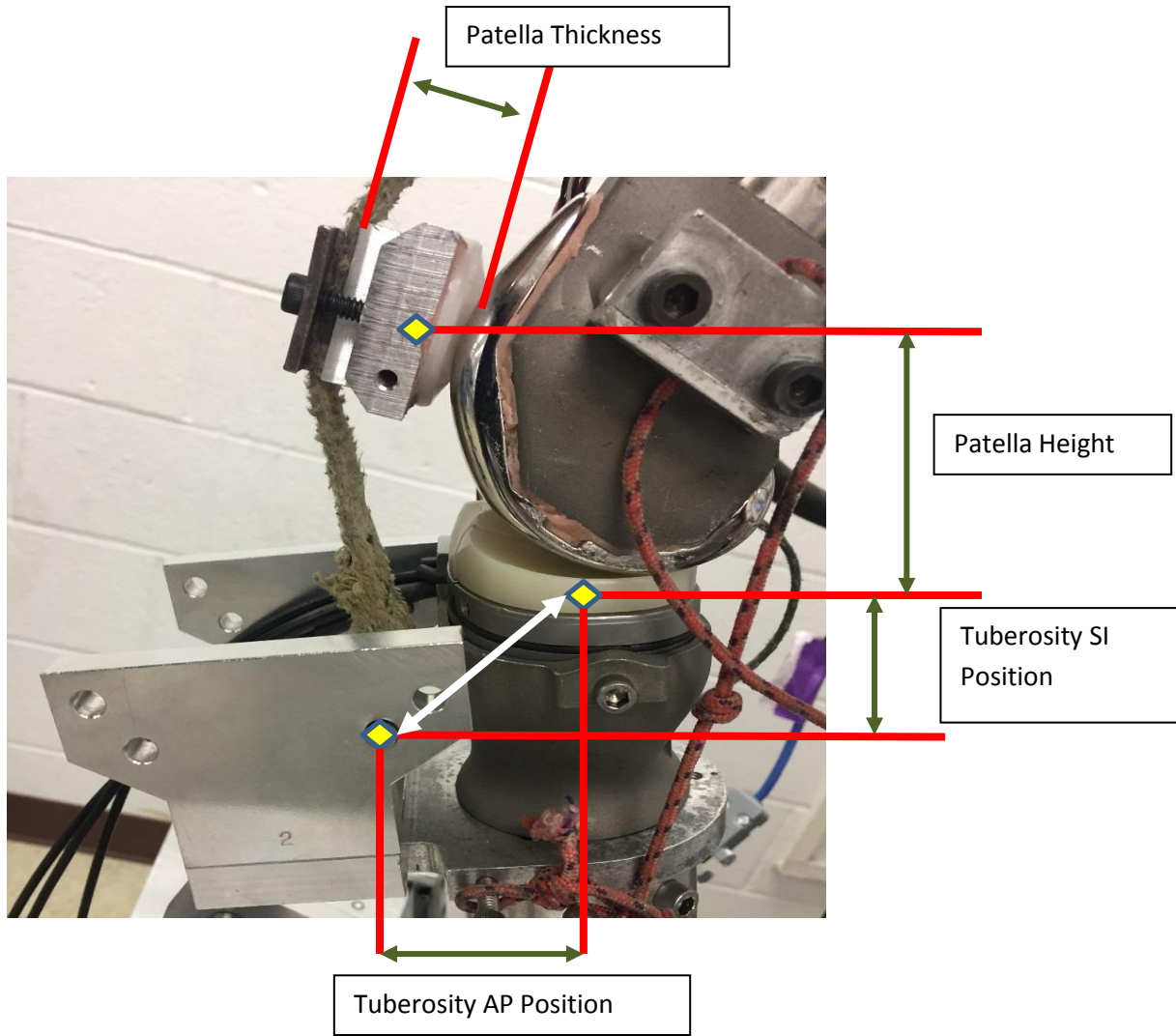


Figure 5: Physical set-up of analog components in the KKS. The components being used for this experiment are Primary Attune (DePuy Synthes), Sz 8. Patella height and tibia tuberosity position measurements are made from an origin located on the tibia plateau at the midpoint between the medial and lateral tibia condyles. Patella thickness is altered using fixed width inserts placed between the patella composite and the Kevlar strap (representing the patellar ligament).

3.3.Results

3.3.1. Tibiofemoral AP Load Evaluation

A DOE analysis commonly aims to do three things, determine a desired factor level setting based on minimizing loss, calculate sensitivity of each factor, and predict results of the desired levels. In this study loss is represented by the RMS error, with a desired target value of zero. Levels with the greatest signal-to-noise (SN) ratio are selected as the desired levels for each factor. A higher SN ratio relates to

reduced normalized RMS error in TF-AP load. Peak SN ratio for patella height occurs at factor level one and three, for the WalkDOE and simple squat profile respectively. Peak SN ratio for patella thickness and tuberosity position occurs at factor level three and level one respectively, Figure 6. Patella thickness and tuberosity position show the greatest sensitivity to minimizing total RMS error for the walk and squat profiles. Patella height has a much lower sensitivity to the RMS error of TF-AP load, Table 2. The resulting desired configuration reduced the RMS error of total AP loads compared from the previous analog configuration from a value of 71.95 lbs to 4.76 lbs, Figure 7.

Table 2: DOE factor sensitivity for walk and squat profiles, and peak SN ratios.

Factor	Sensitivity (dB ²)		Peak SN Ratio (dB)	
	Walk	Squat	Walk	Squat
Patella Thickness (PT)	41.49	74.89	7.2	13.1
Patella Height (PH)	2.53	1.75	5.5	10.2
Tuberosity Position (TA)	91.46	40.66	9.2	12.5

3.3.2. Kinematic Evaluation

The scree plot for the WalkCAD profile shows that the first five PCs account for 81.5% of the variation in the original data set, Figure 8. The results of the first five PC's were plotted with both recalculated variables after perturbing the PC by \pm three standard deviations, and coefficients of the PC that were color coded based on their magnitude, Figure 9. These plots were used for interpretation of the first five PCs. Of these five PC's, PC-1, PC-4, and PC-5 include correlations between anatomic measurements and kinematics. The remaining PC's included in the analysis show correlations to specific kinematic measurements and/or quadriceps load. Limited variation in the data was explained by any PC beyond PC-5 (< 5%), and will ultimately start representing experimental noise.

The explained variation described by PC-1 (33.4%) correlates changes in patella height and tibia tuberosity SI position with changes in quadriceps load, TF – IE rotation, PF – spin, PF – tilt, and PF – ML translation, Figure 9. Increased patella alta correlated to increased medial patellar shift, medial patellar tilt, internal tibial rotation, and patellar adduction. The explained variation in PC-4 (8.9%) correlates

changes between patella thickness, PF –spin, and PF – ML translation, Figure 21. The relationship shows that as patella thickness increases, changes in patellar adduction increase and patellar medial shift increase, particularly in deep flexion during swing phase.

The explained variation in PC-5 (5.7%) correlates changes between PF – FE angle during swing phase, patella thickness, and tibia tuberosity SI position, Figure 22. The relationship shows that as patella thickness increases, patella flexion increases during swing phase.

A summary of observed correlations for the first five PCs are provided in Table 3. Weak correlations are indicated with an enclosed arrow and the direction of the arrow indicates either an increase (pointing up) or a decrease (pointing down) of the related variable.

Table 3: PC correlation summary and percent explained variation of each PC. Fields with ± are variables with coefficients > 70% of the maximum value, representing strong correlations. Fields with (±) are variables with coefficients >50% and <70% of the maximum value, representing weak correlations. No symbol indicates no correlation. Similar signs show variables are correlated in the same direction where opposite signs show variables correlated in opposite directions. The results are shown for the first five PCs only.

Variables	PC1 (33.4%)	PC2 (20.5%)	PC3 (12.9%)	PC4 (9.0%)	PC5 (5.7%)
Patella Height	(+)				
Patella Thickness				(+)	+
Tuberosity Anterior Position				+	
Tuberosity Inferior Position	(+)				(+)
Quadriceps Load	(-)	+			
Tibia Internal Rotation	+				
Tibia Anterior Translations		+			
Patella Flexion			+		+
Patella Adduction	(+)		(+)	+	
Patella Medial Tilt	+				
Patella Medial Shift	+			-	

3.4. Discussion

3.4.1. Tibiofemoral AP Load Evaluation

The objective of the Design of Experiments was to identify desired levels of the selected factors to minimize the error in total AP load compared to the target load measured in vitro. Based on the SN ratios, Figure 6, both the WalkDOE and Simple Squat profiles show the same trend, resulting in

selections for patella thickness and tuberosity position of level three and level one respectively. The profiles disagree slightly for patella height with the walkDOE results suggesting a desired setting of level one and the Simple Squat results suggesting a desired setting of level three. Since the sensitivity of this factor for both profiles is low, and because a higher SN value represents a better response, the level for patella height is selected from the Simple Squat profile as level 3. This gives an overall desired configuration with patella thickness of 28.3mm, patella height of 44.4mm and tuberosity attachment site 5. Significant reduction in error of measured AP joint load was achieved with the desired configuration when compared to the previous analog component configuration, Figure 7. The remaining error between the target load and the achieved load using the desired configuration could be due to differences between testing with a cadaver and testing with analog components (i.e. soft tissue contributions, tibial slope, etc.), KKS actuator tracking differences, or initial alignment differences.

This desired configuration corresponds to a more proximal/posterior attachment site and increased anterior displacement of the patella ligament (due to patella height and thickness). This position creates a greater patella ligament angle relative to the long axis of the tibia. The increased anterior load applied to the tibia creates the increased posterior loads on the tibia tray that more closely matches the Cadaver Target load. The opposite can be observed with experiment 2 that has the opposite position, with a patella thickness of 20.3mm and the most anterior tibia attachment site. In this experiment the greatest anterior loads are observed. While no studies exist (to the author's knowledge) directly showing the effect of patella ligament angle on TF AP loads, there are studies that indicate this angle is related to TF loads. Increased patella thickness increases the patella ligament angle, significantly increasing anterior tibia displacement and external rotation of the tibia relative to the femur in flexion angles greater than 50° [41]. Anteriorization of the tibia tubercle decreases the patella ligament angle resulting in increased PCL strain. This indicates that there is decreased anterior load on the tibia causing the tibia to move posteriorly relative to the femur increasing the strain on the PCL [9]. In cruciate sacrificing designs a

decreased patella ligament angle could relate to significantly increased anterior tibia joint loads and shear force. Increased anterior force could relate to increased component failure and instability, particularly at deep flexion angles.

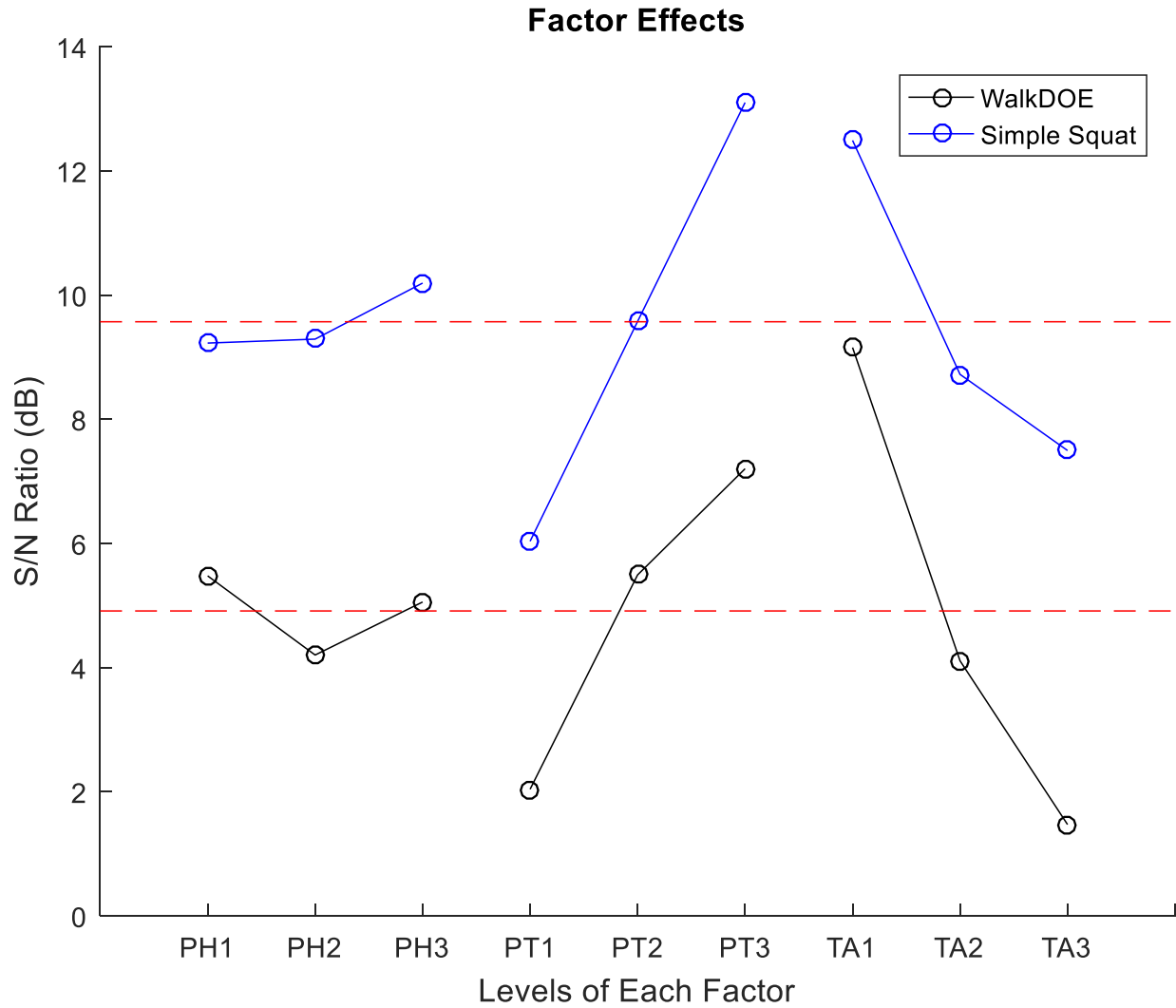


Figure 6: Taguchi Response plot of each factor and level. This shows the average signal-to-noise ratio for the normalized RMS error of AP load between experimental and Cadaver Target AP loads from all three experimental trials. The maximum SN ratio of each factor identifies the level that minimizes the RMS error and corresponds to the desired level for each factor.

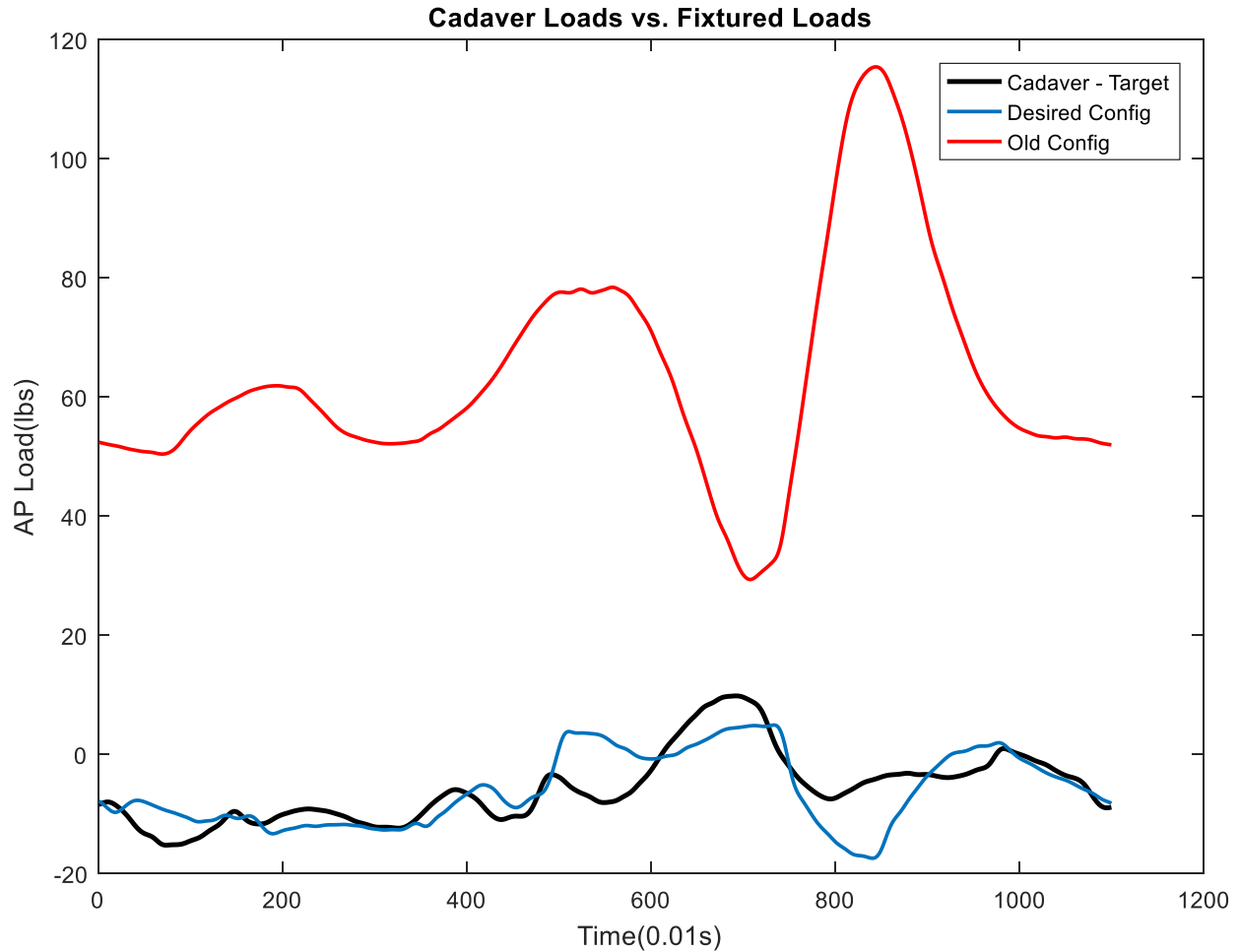


Figure 7: Improvement in achieving Cadaver Target AP loads with the new, desired configuration determined from the DOE, compared to the old analog configuration for the WalkDOE profile. RMS error of total AP load decreased from 71.95 lbs to 4.67 lbs.

3.4.2. Kinematic Evaluation

The objective of this section was to identify the relationship between natural knee kinematics and the three anatomic measures, tibia tuberosity (relative to tibial plateau), patella thickness, and patella height. The greatest variation in the data was explained by PC-1, and describes effects correlated to patella height, Figure 9. The signs of the coefficients reveal that as patella height increases, patella medial shift increases throughout the gait cycle. In cases of patella alta, the patella is initially in a more lateral position [54][55][56]. The lateral position of the patella may, in part, explain the observed correlations in the first PC. One explanation presented by Mizuno et.al. [93], suggests that the

correlation between patella height and observed kinematic changes are all related to a change in Q-angle (angle between the line of the patella and anterior superior iliac spine and a line between the tibia tuberosity and the patella). A higher and more lateral initial position of the patella results in a larger medial shift of the patella as the trochlear groove is engaged. This increases the observed range of Q-angle through flexion. This results in greater medial patella tilt, as the patella is articulating along the lateral edge of the trochlear groove, and greater tibia rotation, from an increase in medial force acting on the tibia [93]. This motion may also contribute to increased lateral contact pressure on the patella. The increase in lateral pressure that occurs on the distal pole of the patella in early flexion would increase patellar adduction (distal pole rotating medially) [3][66]. The change in Q-angle can also be influenced by the ML position of the tibia tuberosity. While this measurement was not included in this analysis, it has shown similar effects on PF kinematics and is an important indicator regarding patellar stability [10].

The relationship between increased patella height and decreased quadriceps load at early flexion angles (<60°) are consistent with previously reported results, where a mechanical advantage exists in early flexion [63]. The advantage exists due to the patella resting in a more anterior position prior to being engaged in the trochlear groove. The change in quadriceps load may also be related to tuberosity SI position. The combined correlation of increased patella alta and inferior tuberosity position (an increase in SI value, Figure 9) may contribute to improved mechanical efficiency by moving the applied force further away from the axis of rotation, even at the cost of reducing the patella ligament angle. The benefit of an increased patella ligament angle to reduce quadriceps load has been observed using the Maquet procedure by anteriorization of the tibia tubercle. This procedure has resulted in greater mechanical efficiency, especially at low flexion angles [5][8][9][87].

In PC-2, an increased change in quadriceps load is correlated to an increase in anterior tibia motion. A more anterior tibia position decreases the mechanical advantage of the extensor mechanism

explaining the increase in quadriceps load [75]. This correlation may also be related to the contribution of soft tissue structures, like the ACL, and passive geometric constraint, that limit the amount of AP motion under compression. This relationship is likely to affect AP shear forces at the tibia plateau as well.

The correlations observed in PC-4 are between patella thickness, tuberosity AP position, patella spin and patella ML translation. The coefficients of patella thickness and tuberosity AP position have the same sign, meaning an increase in patella thickness correlates to an increase in tuberosity anterior position. Increases in anterior position have been shown to decrease PF joint load and stress at knee flexion angles below 90° [5][8][9] [87], with the greatest reduction in load at mid flexion between 45° and 60°. It is in this TF flexion range (swing phase) that the greatest correlation exists. The reduced contact stress in the lateral and medial facets may contribute to increased patella medial translation and adduction. There are no studies that have looked at the effect of tuberosity anteriorization on PF and TF kinematics that would help to explain this correlation. The correlation between large patella thickness, increased medial shift and adduction of the patella are consistent with previous studies that show large patella thickness results in a more lateral patella in early flexion [18][37][38]. This initial lateral position would require increased medial shift and would put a larger lateral load on the distal pole of the patella and increase patellar adduction.

The correlations observed in PC-5 are primarily between patella flexion and patella thickness. The correlation between patella thickness and the patella flexion angle relates to changes in patella ligament angle. Increased patella thickness without a corresponding change in tuberosity position will result in a greater patellar ligament angle. A greater patella ligament angle will result in a greater proportion of the load in the patella ligament to be directed posteriorly. The greater posterior force acting on the distal pole of the patella will increase the patella flexion as the trochlear groove becomes less

constraining in mid-to-late flexion. While PC-5 explains very little variation in the data, it still provides a specific, meaningful relationship that would have been difficult to observe in traditional data analysis.

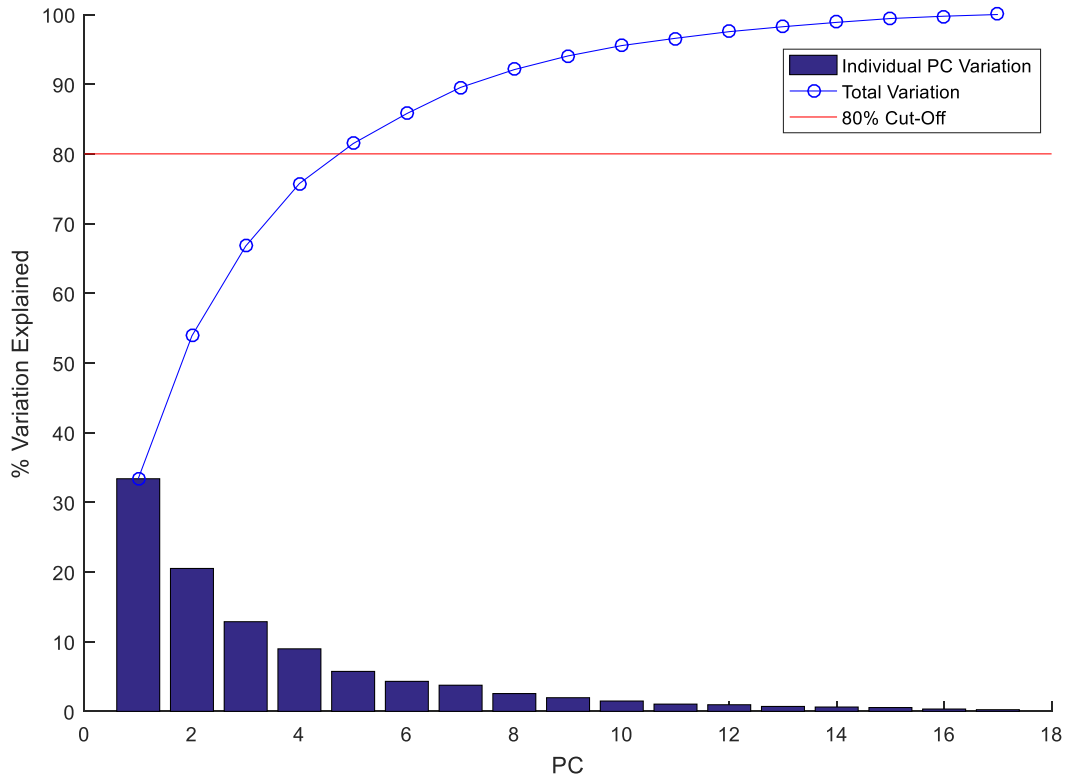


Figure 8: Walk Profile scree plot of both individual PC and total explained variation. Subsequent PCs are used for analysis until a threshold of 80% total explained variation is reached. This plot shows that including the first five PCs will achieve 80% total explained variation and are the only PCs used in the analysis.

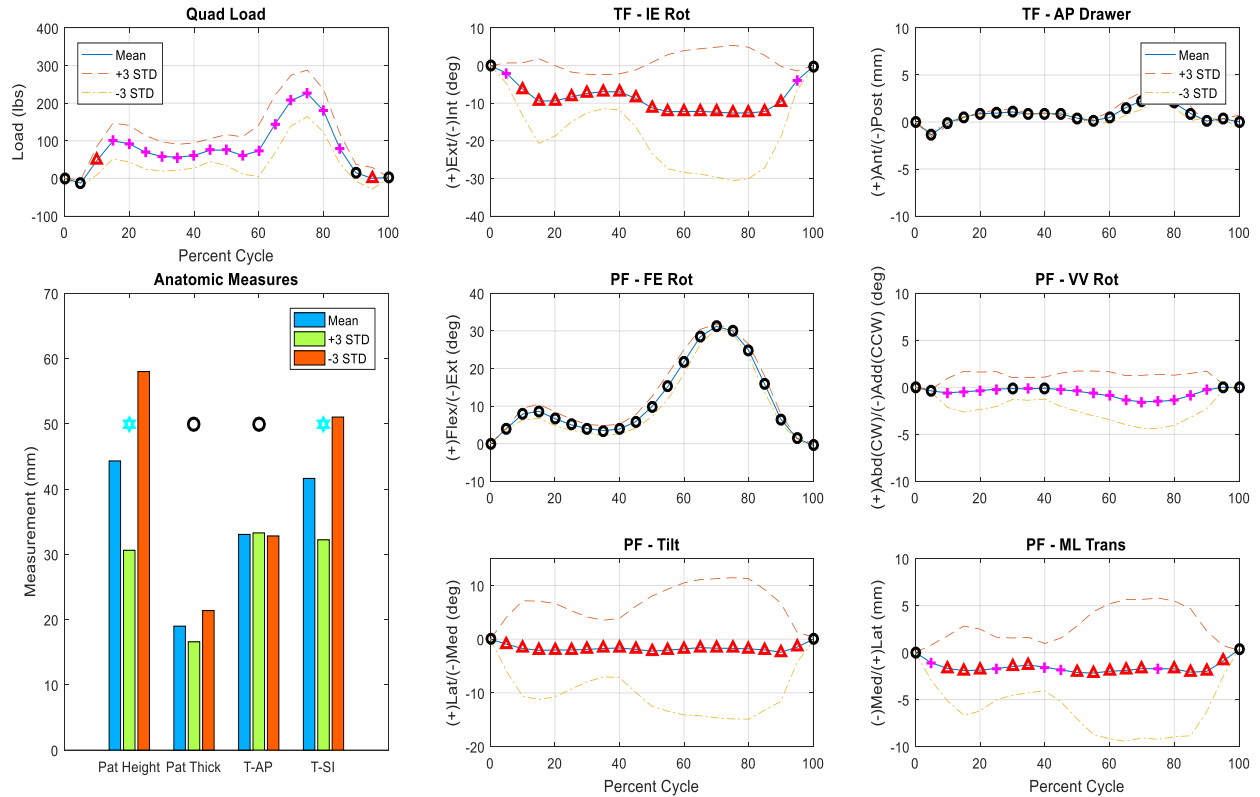


Figure 9: Walk Profile - PC1 (described 33.38% of data variation). Plot includes all variables of the mean and after perturbing PC1 by ± 3 standard deviations. The coefficients for each variable are color coded along mean data line (blue colors are negative coefficients, red colors are positive coefficients). Bright red and dark blue represent strong correlations (70% of max/min) and magenta and light blue represent weak correlations (50%-69% of max/min). Quadriceps load is shown in the upper left corner, TF IE rotation is middle-top and TF AP translation is upper-right corner. The bottom 4 plots are PF kinematics, FE, VV, IE, and ML motion from left to right, top to bottom respectively. The geometric measurements of patella height, patella thickness, and tuberosity position are shown in the lower left corner. The same plot configuration was used for the four remaining PCs included in the analysis.

3.5.Conclusion

The first objective of this study is to determine a desired configuration of the analog components assembled in the KKS that will more closely match Cadaver Target TF-AP joint loads. The ability to match joint loads allows for development of dynamic simulation profiles using analog components, rather than the use of cadavers, which can be costly, time consuming, and prone to failure. Total AP loads were measured using a custom ITT developed by DePuy Synthes. A design of experiments was established to select the desired levels for three factors, patella thickness, patella height, and tibia tuberosity position. The analysis from this study determined that patella thickness and tuberosity position were the most

sensitive factors affecting total AP joint load at the tibia. The desired configuration of the analog components that minimized total TF-AP load RMS error is a patella thickness of 28.3 mm, patella height of 44.4 mm and tuberosity position at 40.6 mm anterior and 29.3 mm inferior to the center of the tibial plateau. This configuration reduced the computed RMS error in the walk profile, WalkDOE, from 71.95 lbs in the old configuration to 4.67 lbs. The desired configuration maximized patella ligament angle, increasing the anterior load applied to the tibia, creating greater posterior loads.

The second objective of this study is to determine how patella height, patella thickness, and tibia tuberosity position, correlate to natural TF and PF kinematics and quadriceps load. Principal components were used to analyze the variation in the data for correlations between variables. The first PC explained 33.4% of the total variation and identified correlations between changes in Q-angle due to patella height and increased medial patella shift. The altered Q-angle is correlated to changes in quadriceps load, tibia IE rotation, patella flexion, patella spin, and patella tilt. The remaining PCs showed correlations to specific kinematics and anatomic measures at decreasing amounts of explained variation. Patella height is associated with the greatest explained variation and is correlated with a majority of kinematic descriptions. This implies that changes in joint kinematics, specifically PF tilt, spin, and ML translation, and TF internal rotation, are more sensitive to variation in patella height than tibia tuberosity or patella thickness.

The DOE results show changes in joint load due to alteration of the patellar ligament angle. The results of the show that TF AP loads are strongly affected by this angle, with large sensitivities for patella thickness and tuberosity position. The sensitivity of patella height on TF-AP loads is low. The PCA results show correlations related to the patella ligament angle in PC-4 and PC-5, which account for a small amount of the total explained variation. This suggests that the patella thickness and tuberosity position (and resulting patella ligament angle) has a greater effect on TF-AP joint loads than it does on TF and PF kinematics. The correlations associated with explained variation in PC-1 are described by

altered Q-angle due to variation in patella height and greater medial patella shift. The correlation between patella height and kinematics combined with the low sensitivity of patella height on TF AP loads suggests that patella height (and resulting Q-angle) has a greater effect on natural knee kinematics than on TF-AP load.

A better understanding of the related effects of the three extensor mechanism factors will guide more informed conclusions in both future research, and decisions regarding medical intervention. Surgeons have the ability to manipulate any one of these extensor mechanism factors, most notably during TKA, to improve the quality of life for patients. The presented results may be used to assess associated risks and understand the implication of significant alterations to the extensor mechanism prior to any surgical intervention. This may also inform the development of new prosthetics or surgical tools. Designs aimed to minimize deviation from natural morphology during TKA may result in fewer mechanical related failures.

The patella height, as discussed in this study, is measured from the center of the tibial plateau. However, the effects due to variations in patella height are related to the patella position relative to the femur. Conclusions about patella height applied to knees after TKA must be aware of joint line shift. Patella alta after TKA that is due to joint line distalization may not result in the same correlation to kinematics. The change in Q-angle may only result if the patella is shifted more proximally relative to the distal femur, not relative to an altered joint line.

There are several limitations and sources of error involved in this study. By offsetting the kinematics and loads in the PC analysis, variations due to natural anatomic morphology are missed. For example, knees that may have tibia rotated internally or in a varus position at full extension. Knees with this kind of natural variation may exhibit different changes in motion throughout gait that will potentially skew results of the PCA. Some of the knees included in the PCA were simulated in previous versions of the KKS, prior to several functional modifications. The variation in how the knees were tested may add

variation in the data that was due to experimental methodology. There are also relatively few knees used in the PCA, more knees may capture more anatomic variation that would be more representative of the population. There are also limitations on size of cadavers used for the PCA, which will limit the observed variation in the anatomic measurements. The PC analysis was not conducted with a squat profile since the knees used in this analysis underwent different magnitudes of TF flexion, therefore no significant correlations can be made for late flexion. The analysis for PF kinematics may also be limited due to only loading the vastus intermedius and rectus femoris. There are multiple soft tissue structures that play a role in patella motion that were not accounted for in these dynamic simulations.

There are also several limitations associated with the study. No soft tissue is present in the analog configuration so any effect that those structures might have on TF force are not accounted for. If the knee was improperly balanced in the KKS prior to running the analog fixtures the load distribution at the tibia will be affected. This alignment is difficult to make in the analog configuration.

3.6.Future Work

Future work related to this study may include running a secondary DoE to investigate the ML distribution of both SI compressive load and AP load and identify what anatomic factors are sensitive to those changes. Work can be done to investigate the effect of AP location of the tibia insert on TF joint load as this has been shown to affect the mechanical efficiency of the extensor mechanism and ACL/PCL strain in cruciate retaining knee replacements. The PCA may be expanded with more knees and anatomic measurements of the femur. There have been indications that the trochlear groove anatomy affects patellar motion and stability. The use of iterative closest point and coherent point drift to capture the entire morphology of the bones could be implemented in the PCA model to capture all changes in anatomy. This work largely focused on tibia and patella components of the extensor

mechanism and sagittal plane measurements. There are many more factors related to the extensor mechanism that could be added to this analysis.

Appendix A: Kansas Knee Simulator LabView control system

A1. Introduction and Background

The use of in vitro dynamic knee simulators is a fairly common practice utilized by both researchers and industry. The goal of these dynamic simulators is to replicate physiological motion and joint load at the knee. Typically the selected simulations aim to replicate daily living activities that patients will commonly perform after surgery, including walking, stair ascent/descent, or even pivoting. Even more extreme motions can be simulated as well to replicate an injury such as an ACL tear [95][96][97][106][107]. In vitro studies have the advantage of being able to perform a wide variety of experiments that would otherwise be unethical in live patients, such as soft tissue resection and the use of rigid bone motion capture markers. Combining the advantages of in vitro cadaver studies with the ability to replicate physiological loads provides for a lot of potential research questions to be answered.

There are several different dynamic simulators that are used in research currently, and many are based off of the oxford style rig. While these rigs may have varying designs they all load the tibia, femur and quadriceps while maintaining the degrees of freedom of the knee [94]. Variations in soft tissue loading, orientation, and added loading parameters (varus-valgus, internal-external) all account for differences among simulator design.

Within the Engineering Joint Biomechanics Research Lab at the University of Kansas, the dynamic simulator, referred to as the Kanas Knee Simulator (KKS), is modeled after the oxford style rig (maintains all 6 degrees of freedom). The KKS contains five hydraulic actuators used to control knee joint kinematics and kinetics. The actuators control five separate motions, vertical hip sled allowing for flexion-extension, ankle flexion moment, quadriceps load, varus-valgus moment, and tibial internal-external rotation. These five controlled actuators allow for a large variety of loading conditions at the knee joint. Typically motion is achieved by controlling flexion-extension angle from the quadriceps

actuator (position control) and load control among the other four actuators (with few exceptions). (Note: If cross compensation is running do not change how any of the actuators are controlled from what is mentioned above).

Previously the KKS was controlled using an Instron© control system. There are several disadvantages to using the Instron system. First, it was difficult to reprogram and alter how the simulator was controlled, particularly whenever the simulator underwent design changes. Second, the equipment was aging and becoming more difficult and expensive to trouble shoot and repair, should it ever stop working or become damaged.

In order to address the disadvantages of the Instron system a LabView cRIO (compact real time input/output processor) system was implemented. There are several advantages to using a LabView based system. First, should any electrical components be added or removed from the KKS (i.e. changes in sensors or servo motors) for any reason it is relatively easy to rewire and connect to the available LabView cRIO modules. Second, the ability to access and change the code combined with the available control library provided by LabView allows a multitude of possible control schemes that could potentially improve the overall control of the KKS. The purpose of the section is to review the developed custom LabView control code and system and compare the achieved control between LabView and Instron.

A2. Labview System and Methods

The purpose of this section is to describe the control scheme and custom built LabView code used to control the KKS and the tracking performance compared to the Instron system. The LabView system uses several different modules in order to be able to run all of the actuators and read in values from all of the sensors. There are six modules used for the control of the system. There is one NI9265, analog current output module that sends a signal to the AdAB sled servo motor and activates the solenoid switch that pressurizes the hydraulics. The activation of the AdAb sled requires two channels, one to

push the sled in opposite directions. The NI9269 is a $\pm 10V$ analog voltage output module that sends a signal to the other 4 servo motors. The NI9203 is a $\pm 20mA$ analog input module that reads in the LVDT sensors for the AdAb sled and vertical sled. The NI9237 is a $\pm 25mV/V$ analog input for bridge circuits. This module is suited to be used for strain gage based load cells and reads in the loads for all load cells (since there are only 4 independent channels two of these modules are required). The second NI9237 module provides an excitation voltage to each potentiometer for the hip flexion and ankle flexion. The NI9205 module reads in the signal for the potentiometer.

Each actuator was tuned separately in both load and position control (if both sensors were available for that actuator) for a PID controller using a frequency response. The next step was to tune them in pairs over expected operating frequency and load, where both actuators would be given a sinusoid input signal and tuned again. This was a way to refine the tuning values of each actuator prior to having the simulator running normally. It is worth noting that the AdAb sled is tuned slightly differently. This actuator is wired into a LabView module that outputs current instead of voltage which makes it difficult to get good control for dynamic input and a steady state input using the same PID controller. Therefore, there are separate controllers, one for steady state input and one for running a profile (dynamic input). All PID values for the individual actuators are available in Table 4 and Table 5.

Table 4: Load control PID tuning values for all actuators

Tuning	Quad Load	Vert Load	Ankle Load	IE Load	AdAb Load (dynamic)	AdAb Load (stationary)
P	0.00055	0.02	0.0031	0.015	0.001	0.03
I	0.15	0.5	0.1	0.1	0.001	0.003
D	0.0002	0	0	0	0	0

Table 5: Position control PID tuning values for all actuators for those with active position sensors.

Tuning	Quad Position	Vert Position	Ankle Position	*IE Position	AdAb Position (dynamic)	AdAb Position (stationary)
P	0.03	0.6	N/A	N/A	18	17
I	1	1	N/A	N/A	2	0.5
D	0	0	N/A	N/A	0	0

*IE did not have an active position sensor at time of tuning, will need to be tuned later

There are three actuators that operate in the sagittal plane. The motion and control of a given actuator will affect the control and motion of each of the other two. The quadriceps (controls FE motion), the vertical sled (compressive load), and ankle moment all apply loads in the same plane and all affect FE angle. Thus, the control system must have these signals communicate with each other to ensure that any added motion from one actuator is taken into account at the other actuators. This method is referred to as cross compensation. The cross compensation algorithm can be seen in a process diagram showing the control loop for all of the signals present in the KKS, Figure 10. The applied cross coupling was based off of similar work of position control systems described by Yeh, Ulu, and Lo [108][109][110]. The cross coupling coefficients and control values are given in Table 6 and Table 7.

The sensor signals from the vertical and ankle load are run through a built in LabView, PID specific, FIR (finite impulse response) filter prior to calculating the error signal. This is done to reduce tracking error due to high frequency signal noise.

Table 6: KKS Cross-Coupling Coefficients for the vertical and ankle actuator

Vertical Coefficients	Vertical Value	Ankle Coefficients	Ankle Value
Vq	1.3	Aq	1.3
Vv	1	Av	0.04

Table 7: KKS Cross-Coupling PID values for the ankle actuator signal

Tuning	Ankle CC PID
P	0.0225
I	0.3
D	0

In the comparison between systems, both the WP4 walk profile and squat profile described in section 3.2.1 were run on each controller. Data from each controller was cut to isolate a single profile run. The data from the Instron controller reported output values at inconsistent times and thus had to be resampled over the same profile input times in Matlab (i.e. the input was given at specific time points, and thus to evaluate the output, the tracking values had to be interpolated to match those same time points). The LabView data was output at the same time step as the input profile and thus do not have to be resampled. The sensor data from the LabView system was filtered through a fourth order low pass butterworth filter, using a sampling frequency of one 1000-Hz.

A3. Results and Discussion

For tracking comparison between systems and actuators the RMS error between target and actual values were calculated and then divided by the range of input signals, creating a percent RMS normalized error. The tracking error can be seen visually in Figure 11 and Figure 12 for the LabView and Instron system respectively. The tracking achieved by with the Instron system was able to track target hip angle with an RMS error around 0.55%, whereas the LabView performed at 1.79% and 5.76% for the squat and WP4 pr ofile respectively. The ankle error was significantly improved with the LabView system for the more dynamic WP4 profile, going from 21.95% to 4.52% RMS error. The total RMS error for each system is shown in Table 8.

Table 8: KKS Tracking performance, percent normalized RMS error between the cRIO and Instron control system

Actuator	Walk (WP4)		Squat	
	LabView	Instron	LabView	Instron
Hip Angle	5.76%	0.53%	1.79%	0.55%
Vertical Load	2.45%	2.19%	*N/A	*N/A
Ankle Load	4.52%	21.95%	4.87%	3.67%

*No input target for vertical load in the simple squat profile

The tracking for the hip angle has significantly higher error in the WP4 profile than the squat profile using the LabView controller. This may be due to the profiles running at different speeds. By looking at Figure 11, the majority of the error seems to occur during swing phase. During this phase the flexion of the knee occurs at a higher frequency than the squat flexion (i.e. the walk flexes and extends in a period of approximately four seconds whereas the squat motion occurs in about 20 seconds). This difference in flexion-extension frequency could be the cause for some of the tracking error as the LabView controller performs better at lower frequencies. It is also noted that for the WP4 profile run using the LabView controller, as the ankle tracking was improved the hip angle tracking performance decreased. This may be due to the relationship between these actuators and the cross compensation method being employed.

A potential source for error in this comparison is from the resampling done for the tracking analysis from the Instron sensor output data. The isolated output tracking data from the Instron controller was selected by hand to have the same initial point as the input target profile. In other words, the assumption is that the initial point selected from the output matches exactly with the initial point of the target. This will skew the data and may not show any shift or lag in tracking.

A4. Conclusion and Future Controls Work

The purpose of this section is to review and compare the performance of the KKS tracking using the custom LabView controller to the previously used Instron controller. The cross coupling methods used in the LabView system show reduced ankle load tracking error while running the WP4 profile while

simultaneously increasing tracking error for hip flexion angle. Similar tracking performance was achieved in the squat profile for the hip angle and ankle load actuators. This shows that the LabView system is capable of achieving good control of the KKS. The reduced performance of the hip angle tracking, particularly at a higher rate of flexion-extension, show that the cross coupling controller can be improved and more robust over a wider range of operating parameters.

Future work may include modeling the control system in MatLab, utilizing the suite of control functions to design a more robust controller (use of "sysID"). A higher resolution ankle load sensor may also improve function; large jumps in load readings cause unexpected jumps in tracking ability of the simulator. This could also be due to how the sensor is attached at the ankle and may benefit from a redesign. Improving the speed of the control loop in LabView may also improve tracking. Currently the code is run directly on the cRIO and cycles through every millisecond. By deploying the control algorithm directly to the FPGA (Field Programmable Gate Array) the sampling frequency may be increased, potentially reducing tracking error further.

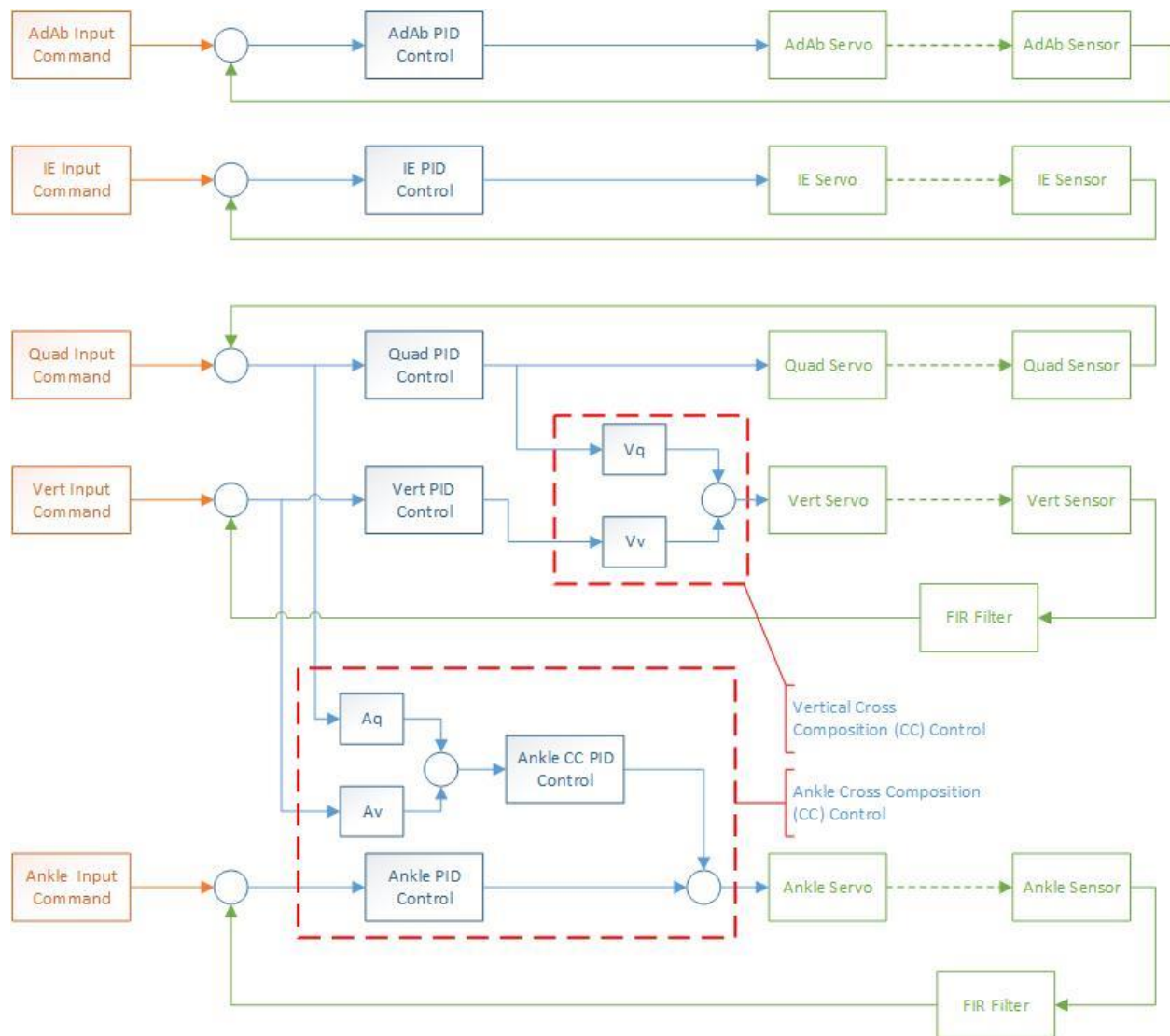


Figure 10: Process Flow Diagram of KKS Controller Utilized in LabView Code. The red boxed components show the cross compensation algorithm used for the vertical load and ankle load actuator.

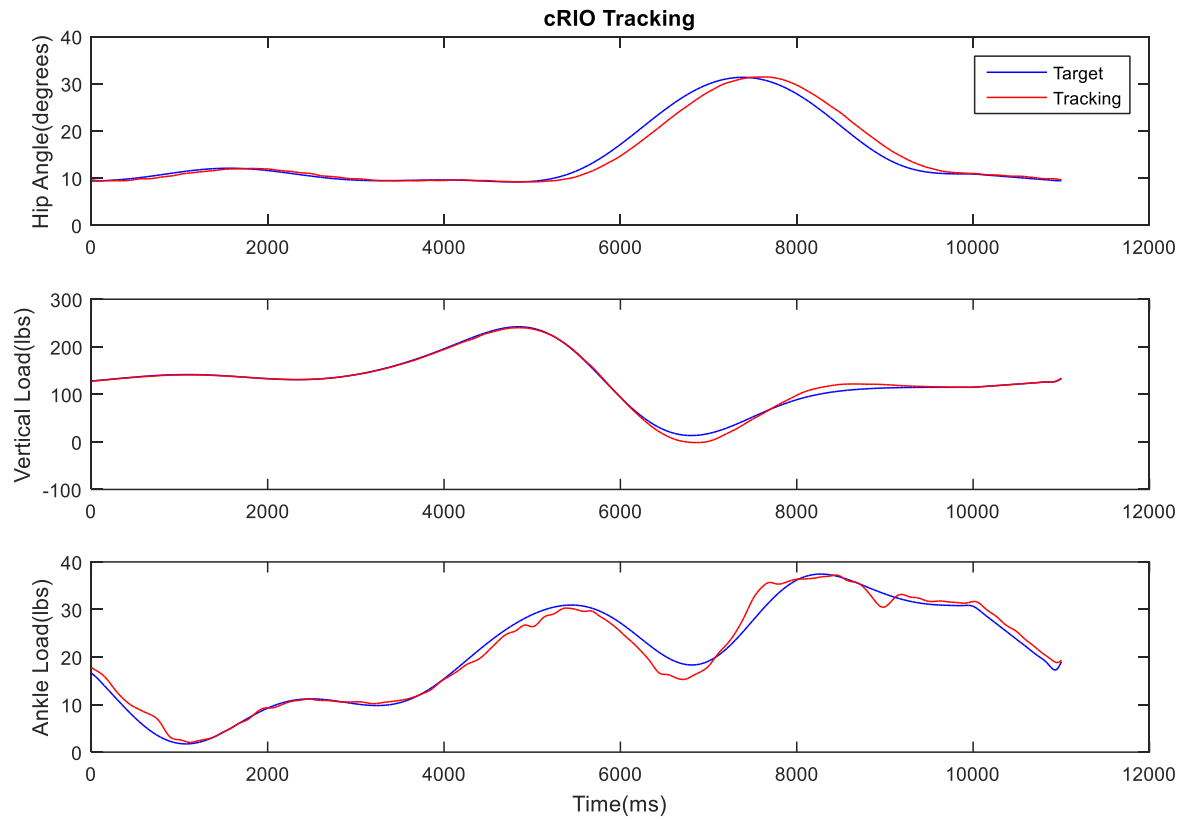


Figure 11: KKS Actuator Tracking Performance using the LabView cRIO system and cross compensation (after filtering sensor signal) applied to the vertical load and ankle load actuators. The profile being tracked is the 'WalkDOE' profile utilized in the TF-AP load evaluation.

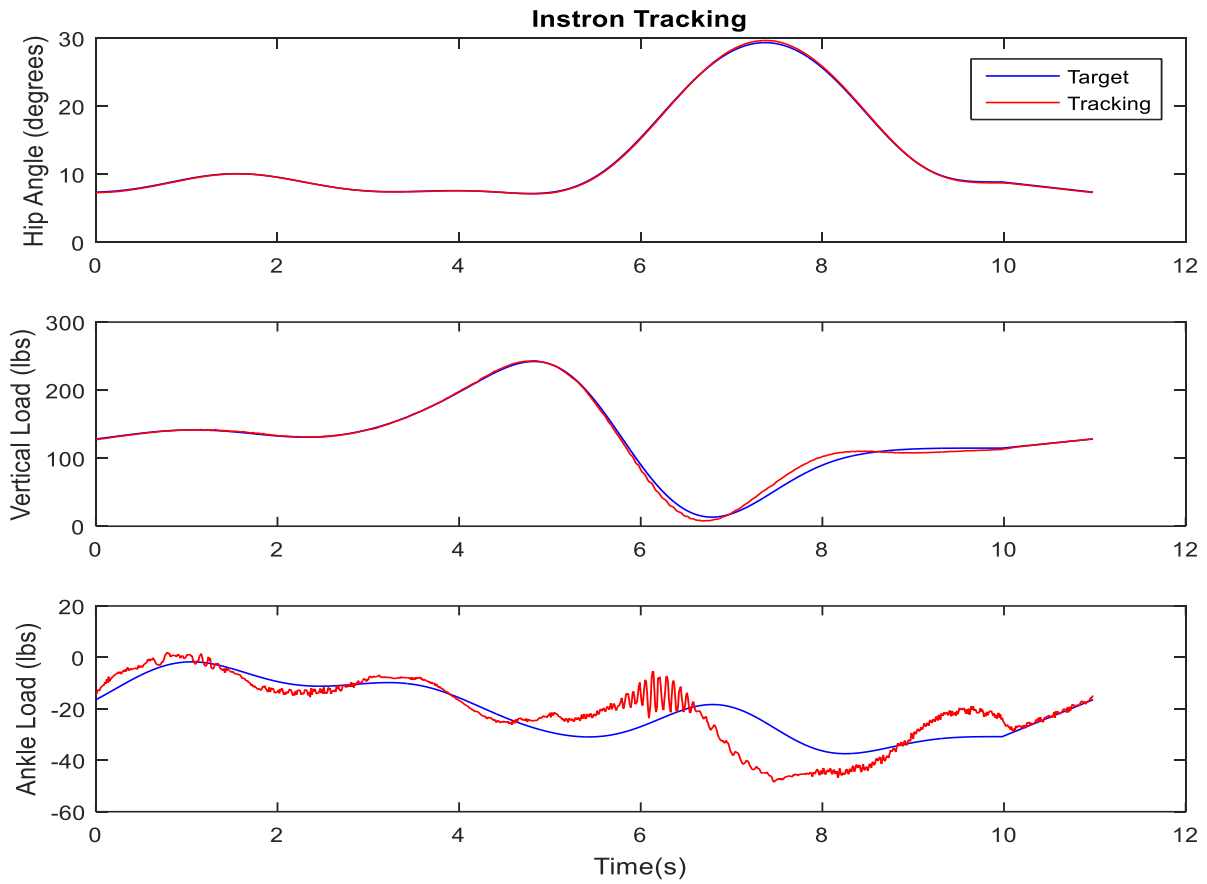


Figure 12: KKS actuator tracking ability using the Instron system. The sensor signals have not been filtered here and the tracking data had to be cut, resampled, and overlaid with the target data. This is due to the tracking data not being recorded at consistent intervals compared to the input target data. This shows the tracking for the "WalkDOE" profile that was used in the TF-AP load evaluation.

Appendix B: Additional Figures

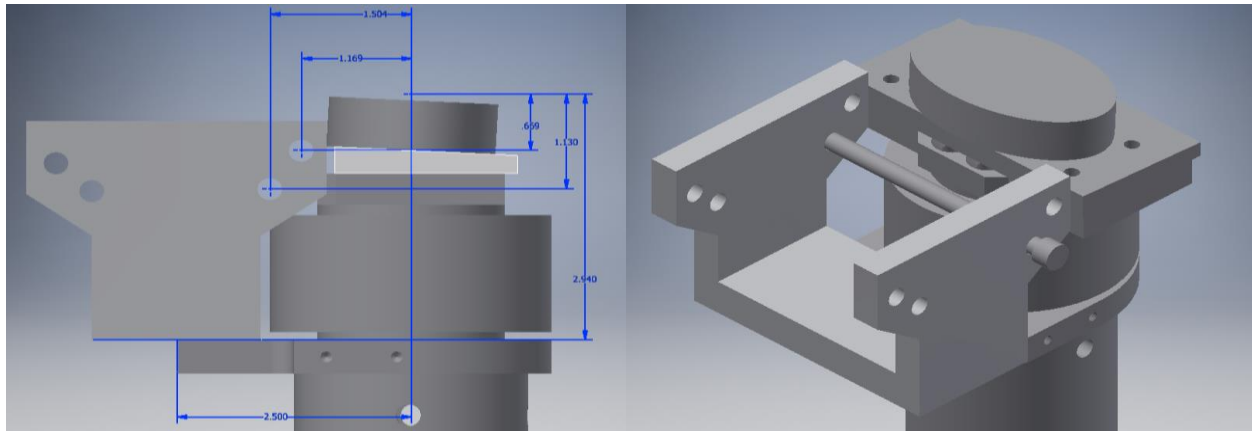


Figure 13: (LEFT) Location of tuberosity positions (sagittal plane, anterior to the left) on the analog fixture relative to the center of the tibia insert. Locations are related to a Sigma total knee replacement sizes that correlate to a certain anatomical sized knee. (i.e. size 2 would be a smaller knee than size 6 and have a more posterior and superior tibia attachment position relative to the center of the tibial plateau). **(RIGHT)** Isometric view of the KKS fixture assembly using the load cell. In these figures, the blue load cell and top plates can be replaced with the ITT and still work.

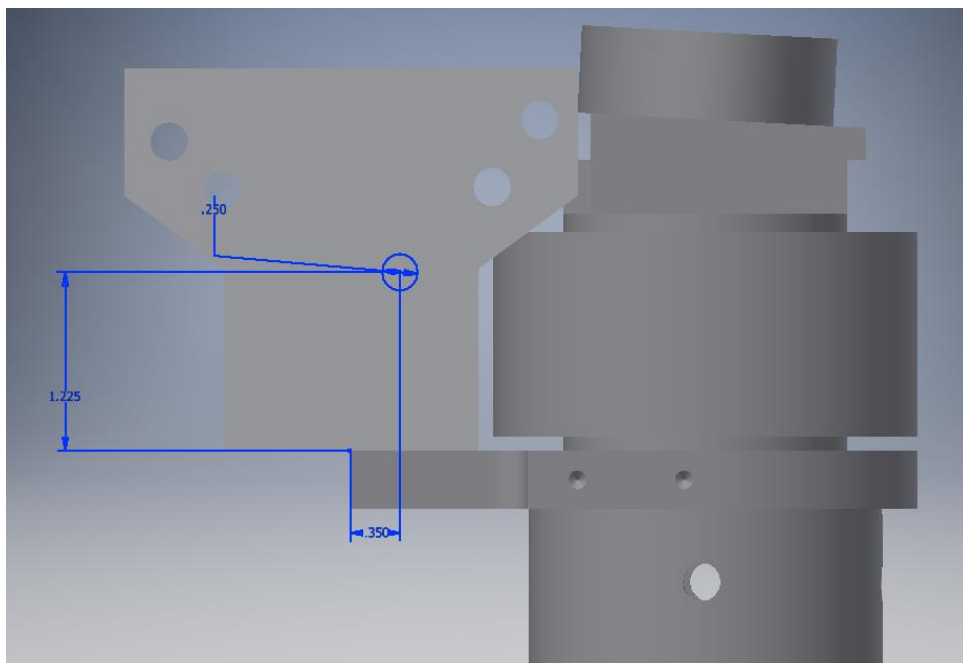


Figure 14: The variable tuberosity positions compared to the original configuration attachment position (blue hole). The associated holes in the above figure are 1.5 (upper right), 2 (upper left), 5 (lower left), and 4 (lower right). To utilize the attachment sites on the left, the attachment fixture would need to be rotated so that sizes 2 and 5 would be closer to the tibia plateau (i.e. only holes on right can be used for tibia attachment positions).

Table 9: DOE Experimental Array corresponding to results obtained in this study.

Experiment No.	Selected Levels		
	Patella Thickness	Patella Height	Tuberosity Site
1	1	1	1
2	1	3	3
3	2	2	3
4	2	1	2
5	2	3	1
6	3	3	2
7	1	2	2
8	3	1	3
9	3	2	1

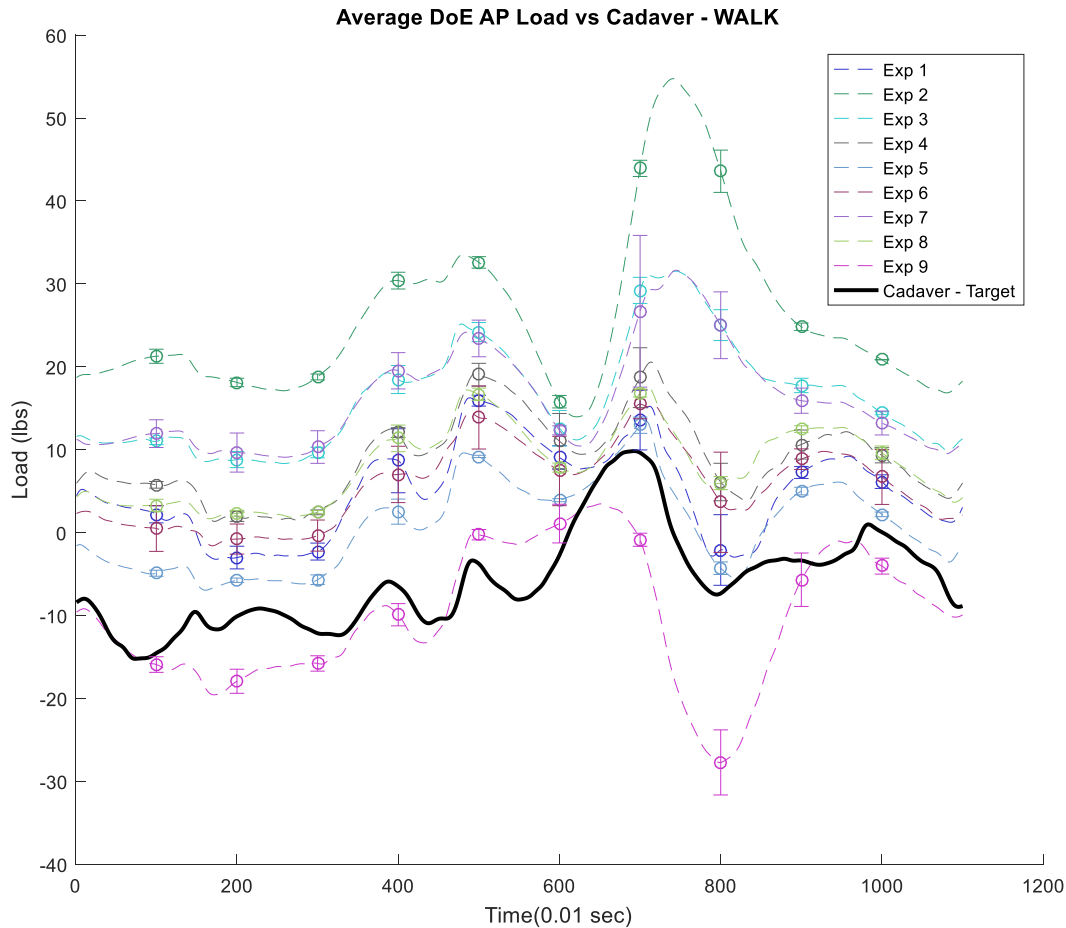


Figure 15: Average total Anterior (+) / Posterior (-) loads of all 9 experiments from the DOE for the “WalkDOE” profile among all 3 trials run. Standard deviation of all the trials is reported every second. The low standard deviation suggests good repeatability between all trials for every experiment with the most deviation occurring in swing phase (the last 4 seconds).

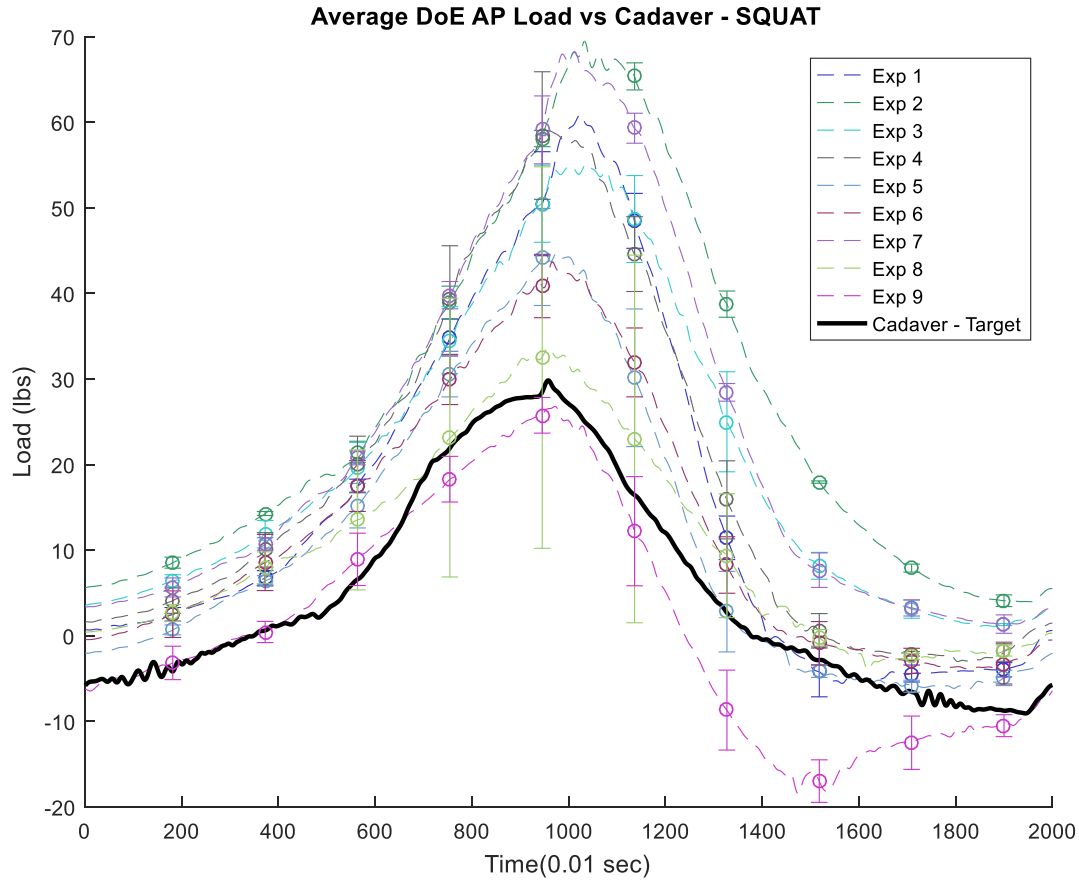


Figure 16: Average total Anterior (+) / Posterior (-) loads of all 9 experiments from the DOE for the “Simple Squat” profile among all 3 trials run. Standard deviation of all the trials is reported every second. The low standard deviation suggests good repeatability between all trials for every experiment.

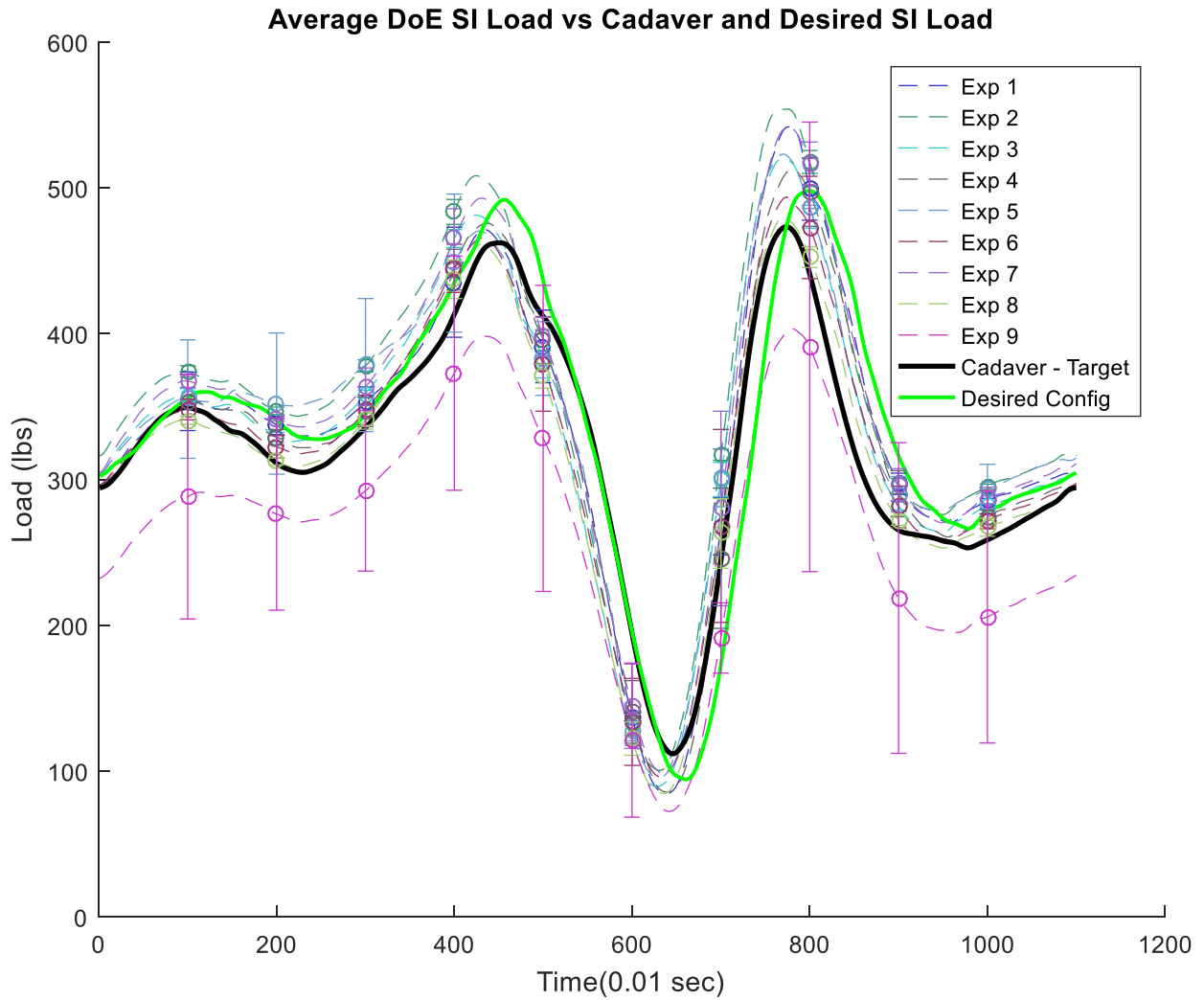


Figure 17: Average SI compressive forces from all trials of the 9 experiments (dashed lines) for the “WalkDOE” profile. Minimal variation between experiments and trials can be observed. The Cadaver Target data (black) and the desired configuration (green) show good comparison, therefore the desired configuration did not negatively impact SI compressive force.

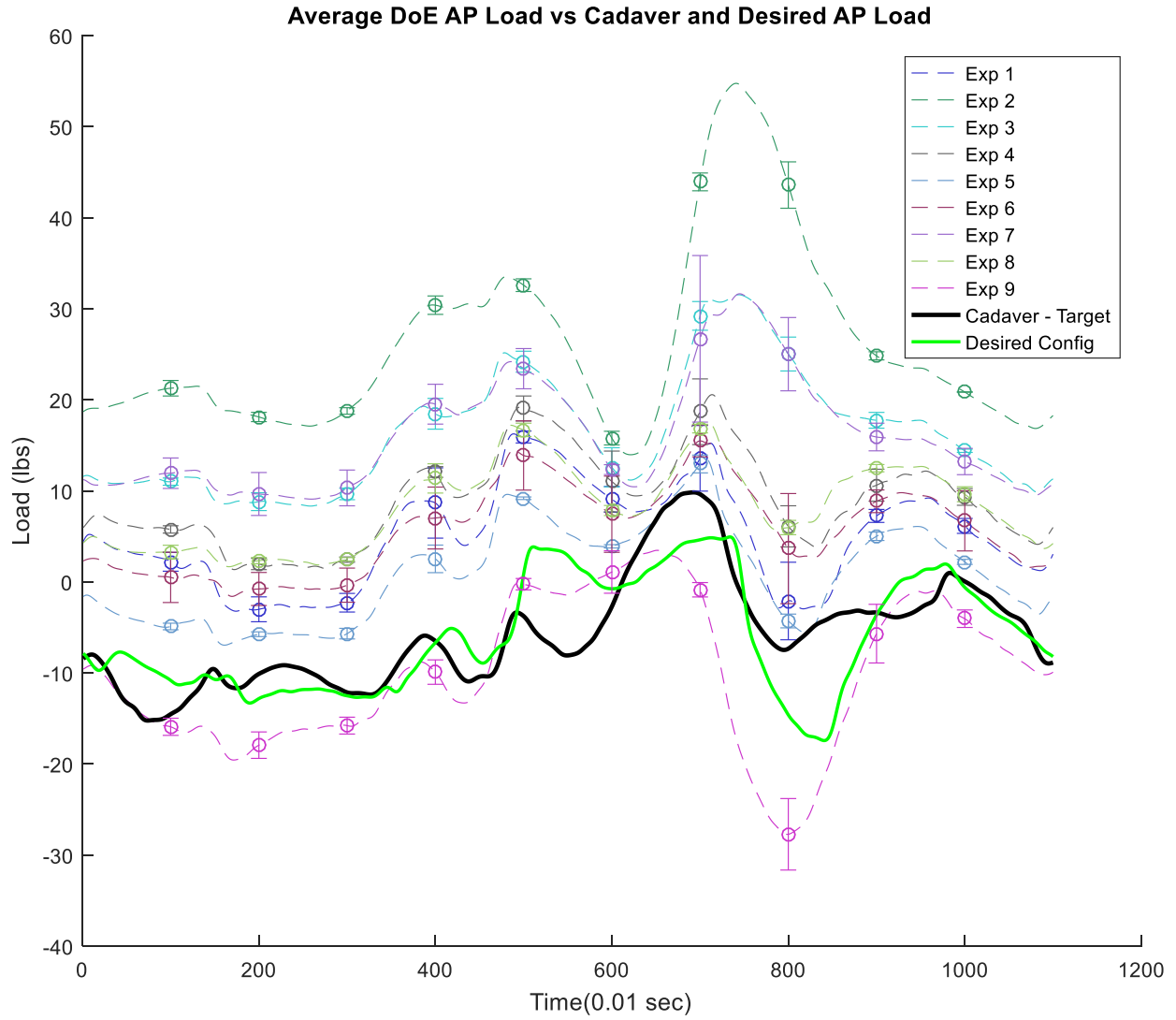


Figure 18: Average AP loads during the “WalkDOE” profile for all 3 trials including the result of the desired configuration setting (green).

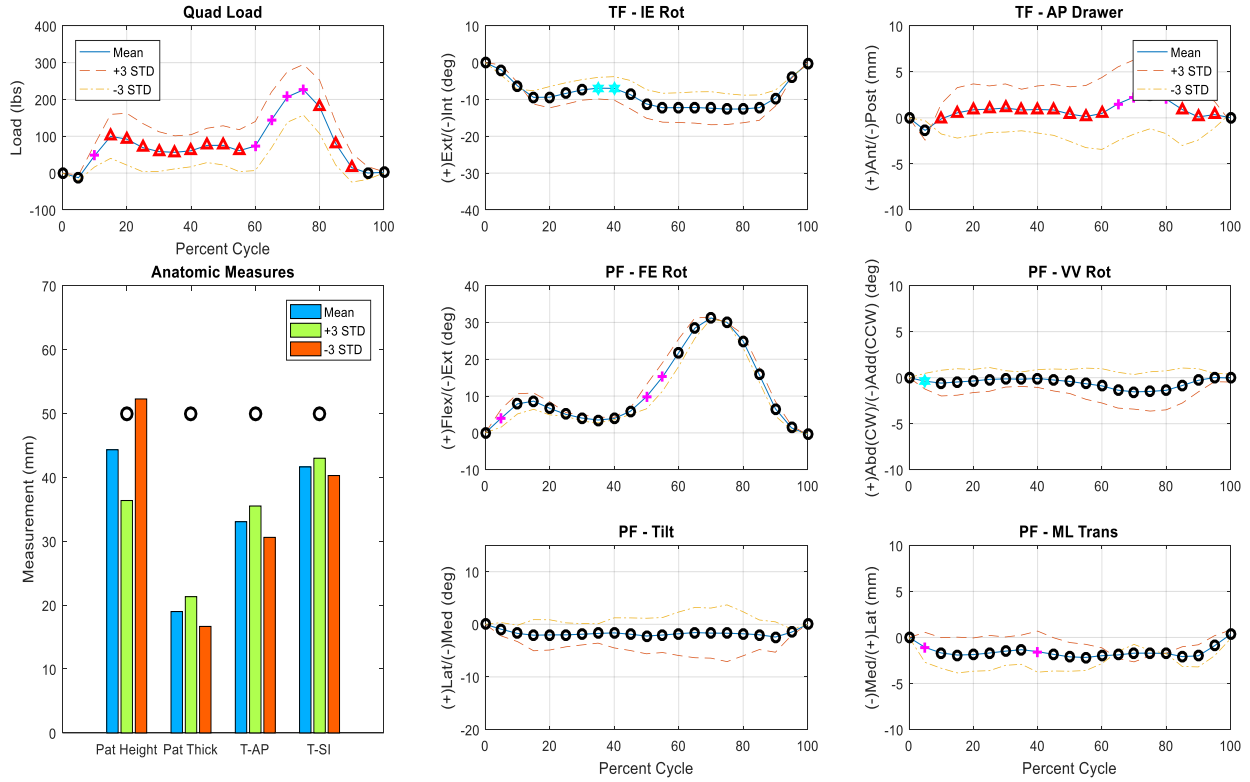


Figure 19: Walk Profile - PC2 (20.51% explained variation).

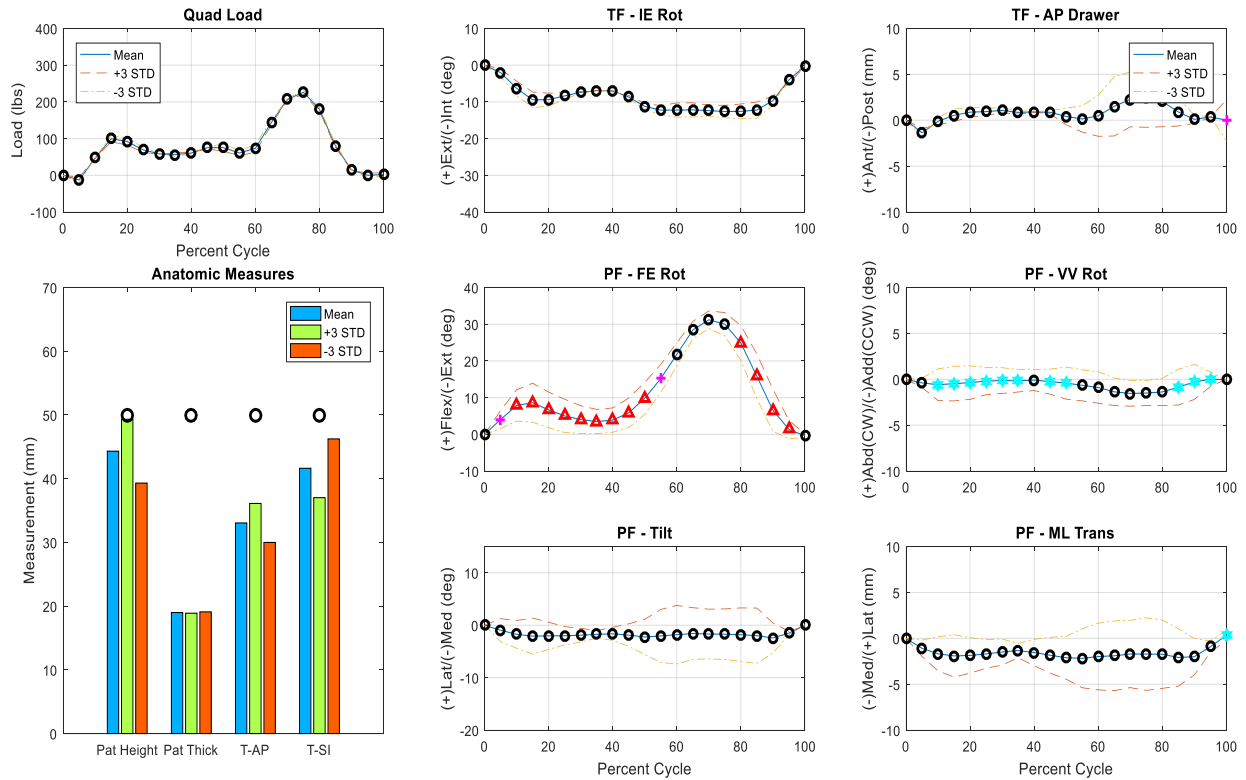


Figure 20: Walk Profile - PC3 (12.87% explained variation).

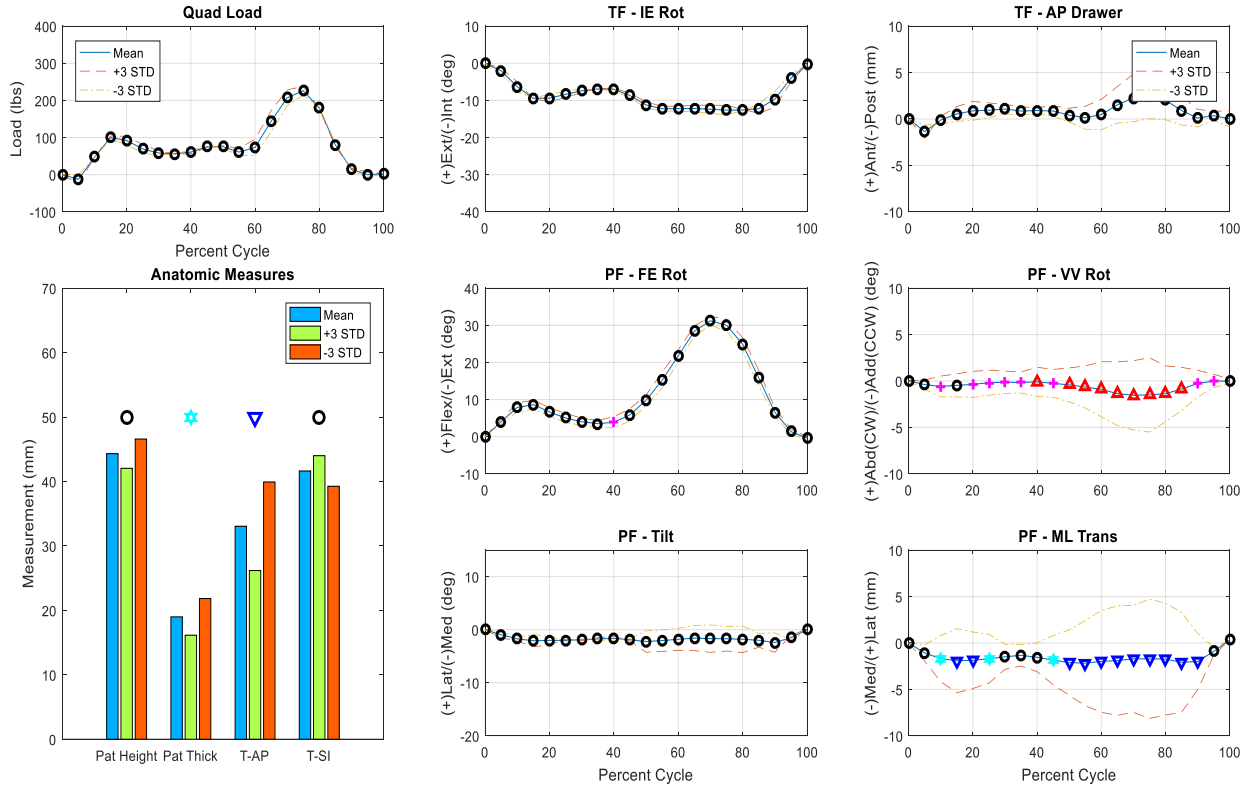


Figure 21: Walk Profile - PC4 (8.97% explained variation).

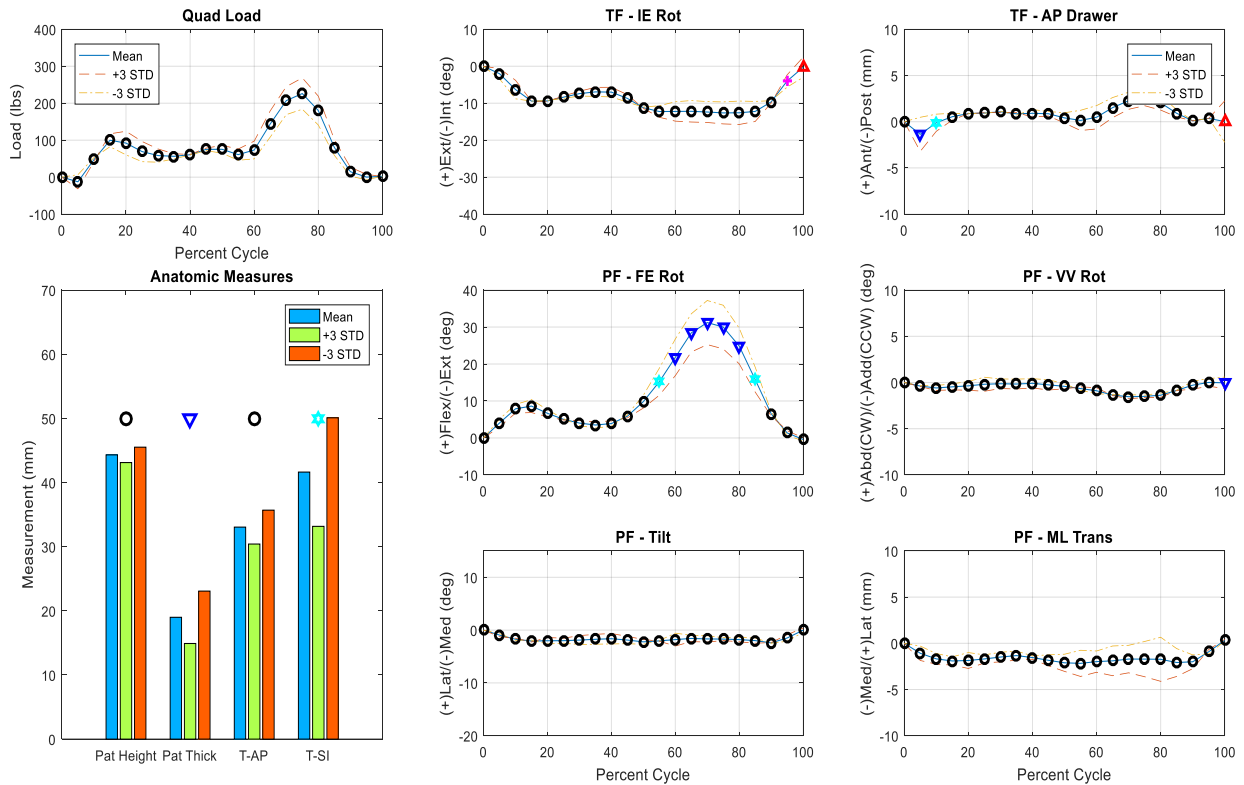


Figure 22: Walk Profile - PC5 (5.74% explained variation). After this PC, more than 80% of variation in original data was explained.

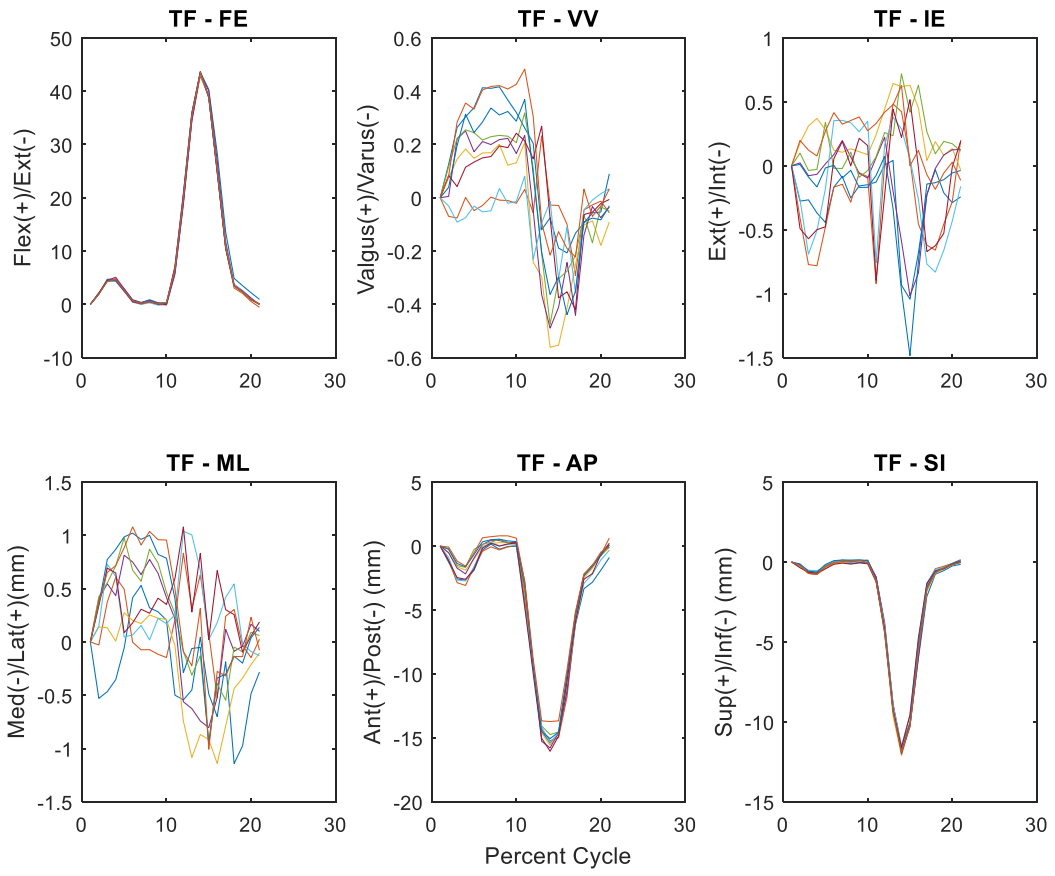


Figure 23: Trial 3 offset TF kinematics for all 9 DOE experiments. Single profile of WalkDOE walk cycle.

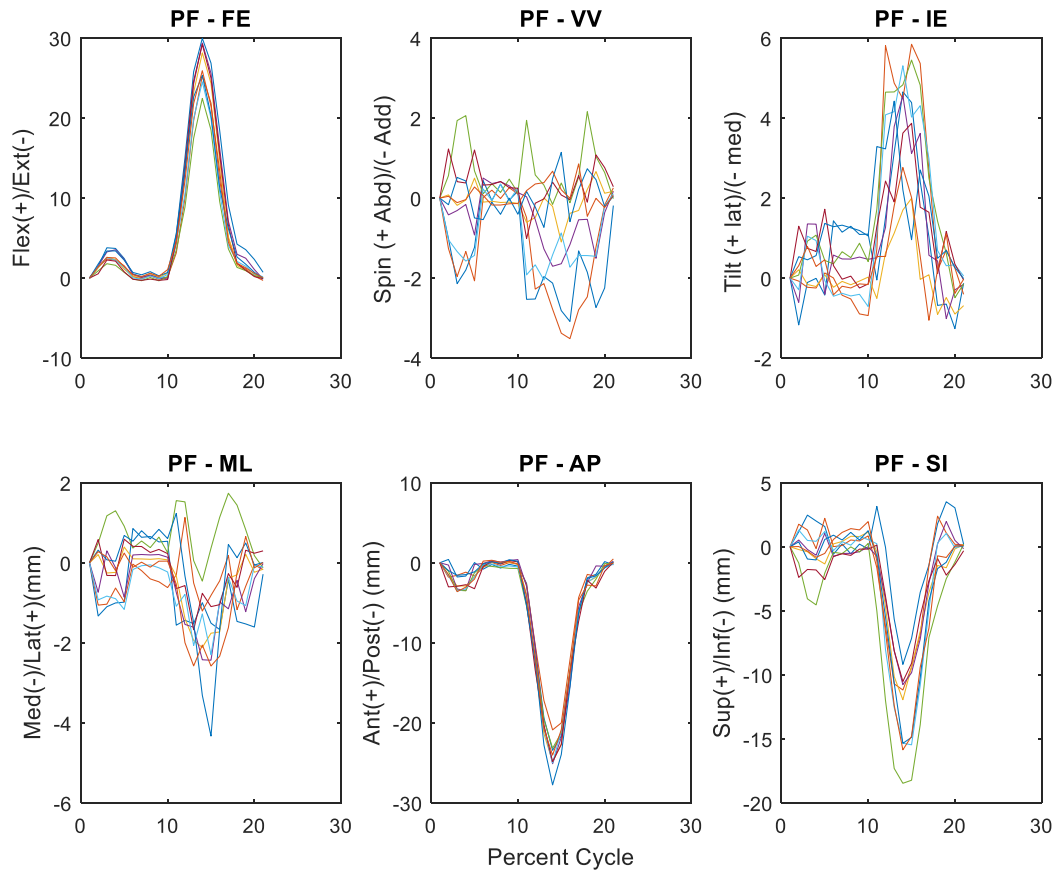


Figure 24: Trial 3 offset PF kinematics for all 9 DOE experiments. Single profile of WalkDOE walk cycle.

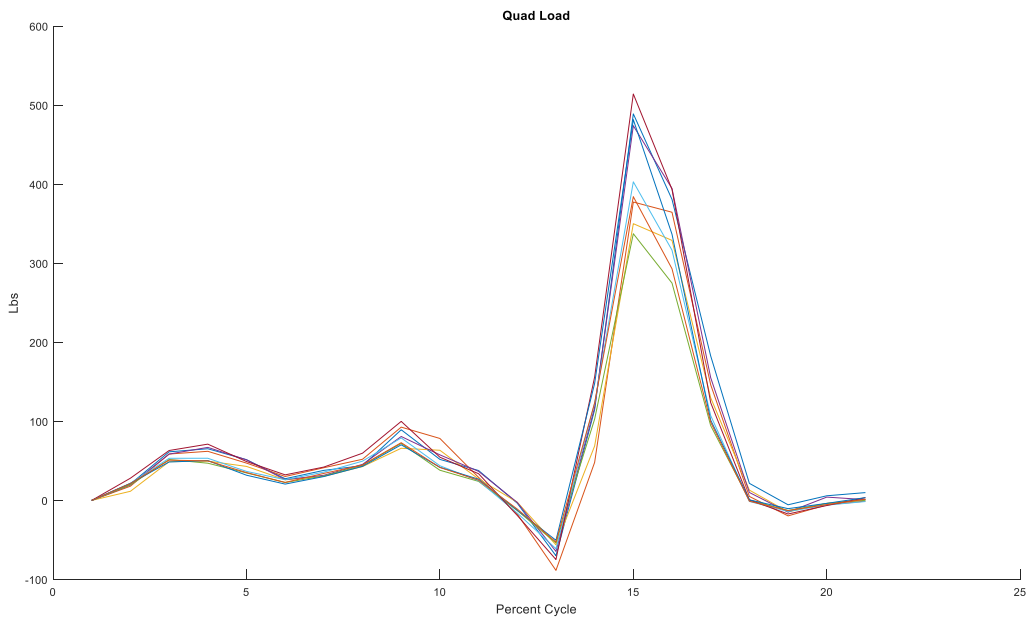


Figure 25: Trial 3 offset quadriceps load measured during a single cycle of the WalkDOE walk profile for all 9 DOE experiments.

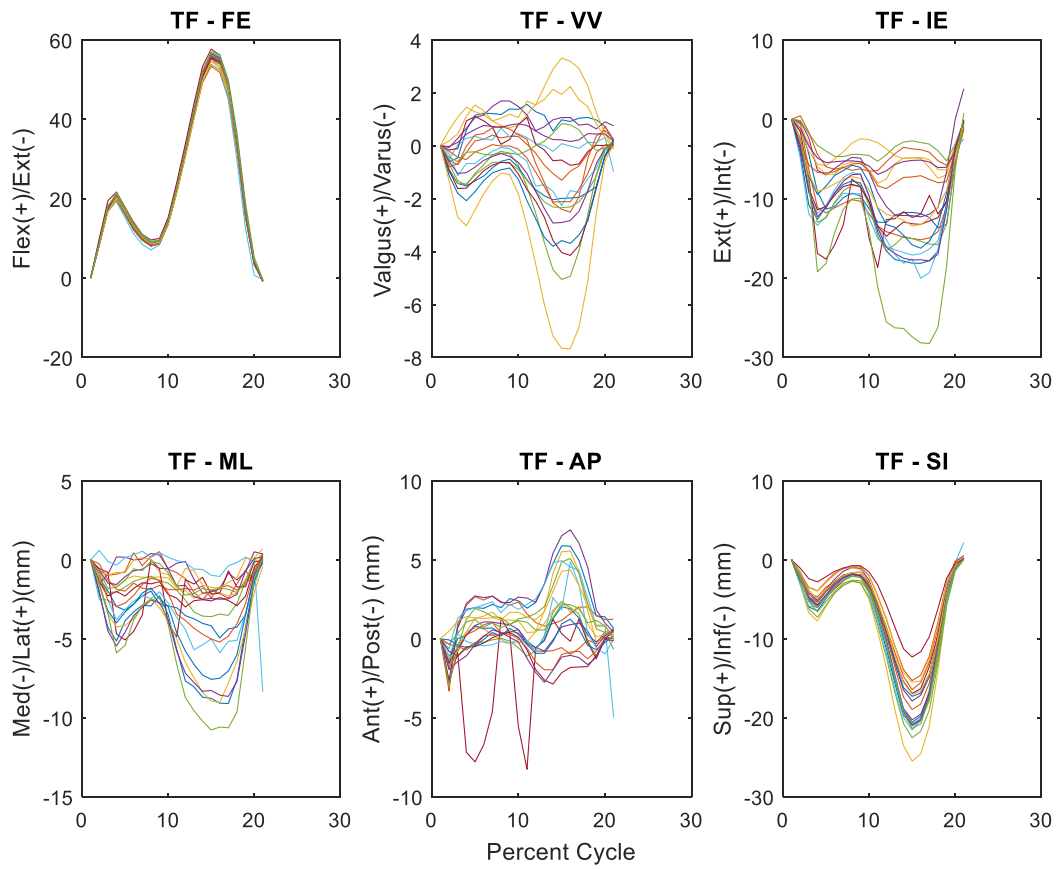


Figure 26: Natural knee offset TF Kinematics of a single WalkCAD walk profile for all 19 knees considered in PC analysis. The red line that varies considerably in the AP translation plot (middle, bottom) is knee number 11 and is considered an outlier and omitted from the PC analysis.

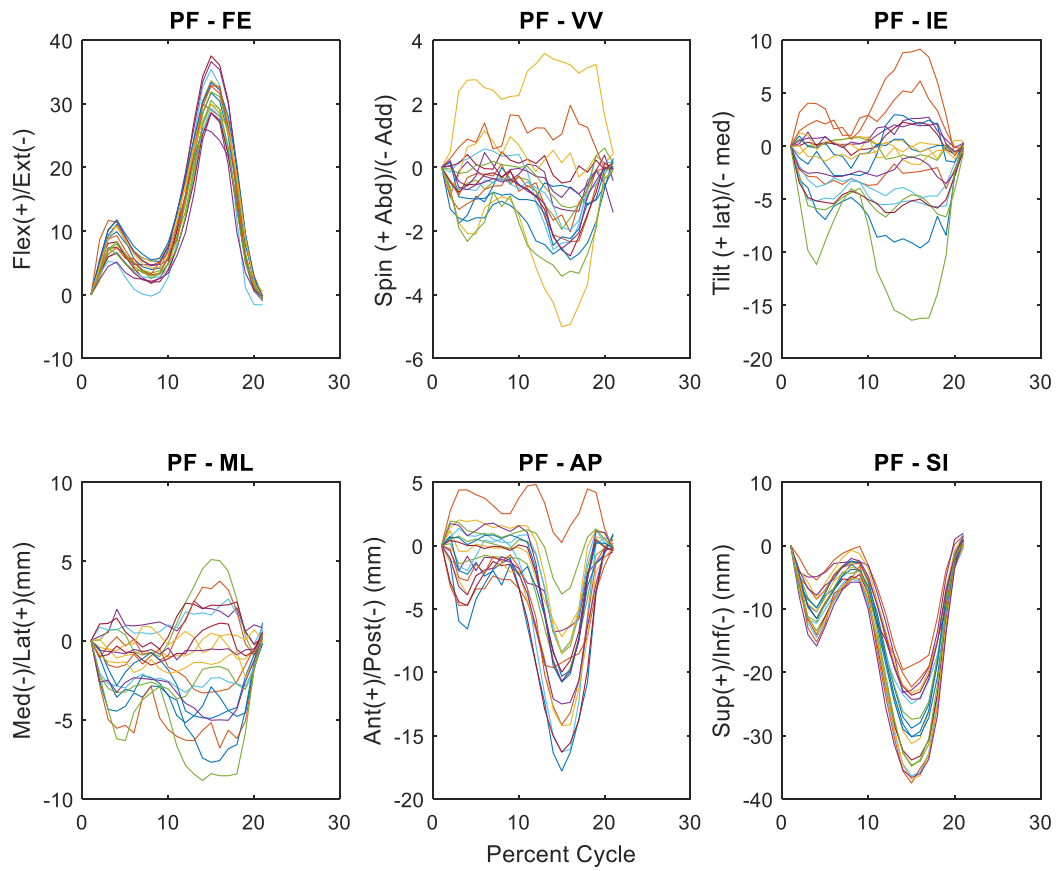


Figure 27: Natural knee offset PF Kinematics of a single WalkCAD walk profile for all 19 knees considered in PC analysis. The same outlier identified in natural knee TF kinematics is removed from the PF data set for PC analysis as well.

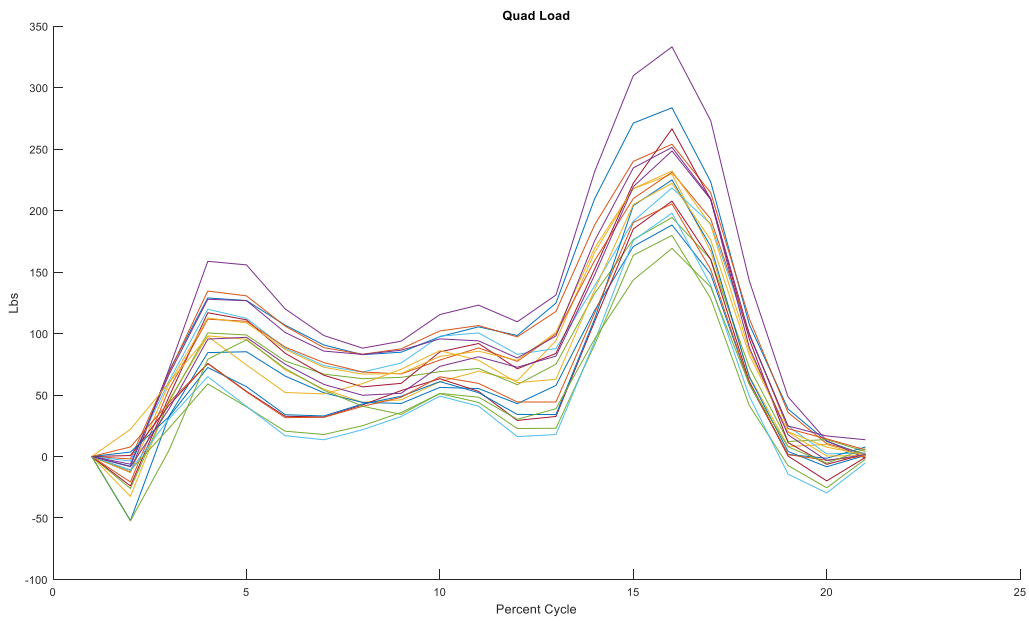


Figure 28: Natural knee offset measured quadriceps load of a single WalkCAD walk profile for all 19 knees considered in PC analysis.

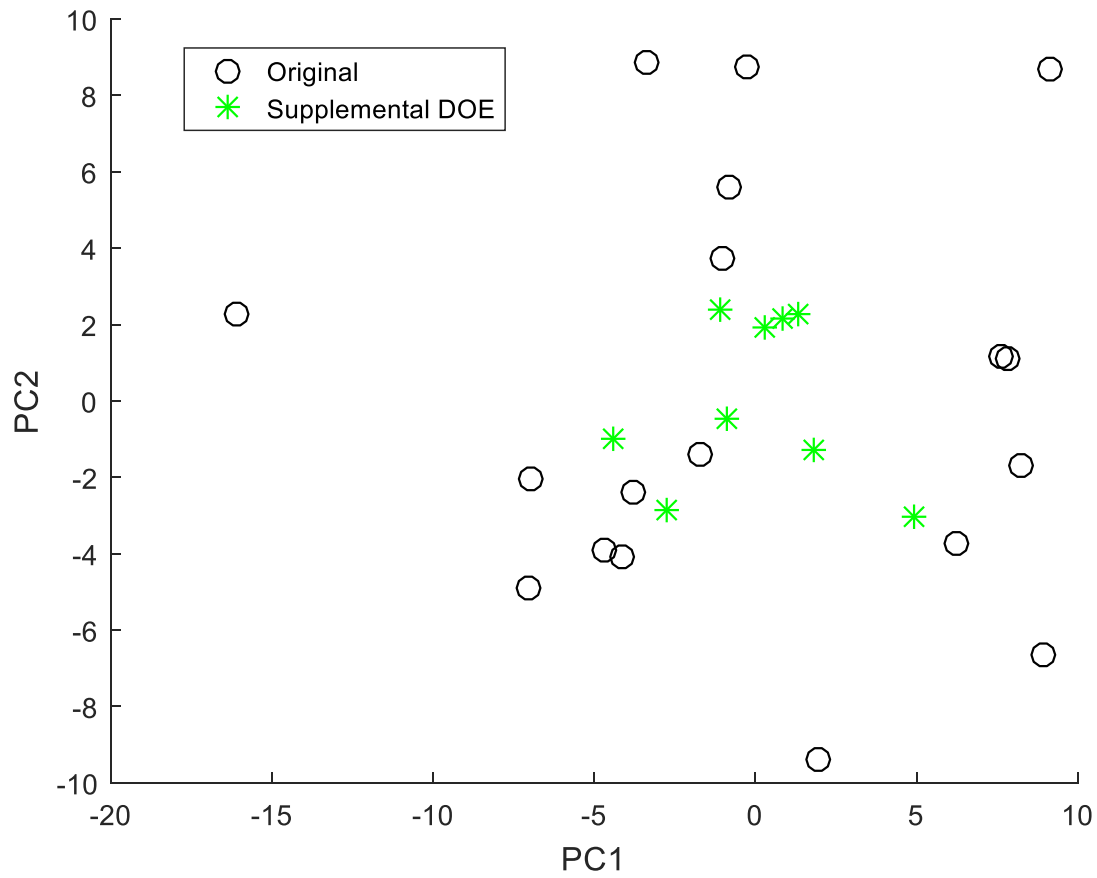


Figure 29: PC1 vs. PC2 scores of the 18 original observations included in the PC analysis of the natural knees (black) plotted against the scored DOE kinematics and quadriceps load (green). The variation of the DOE kinematic data was much narrower than the cadaver kinematic data; however, these two data sets were conducted with different profiles, under different considerations, comparing TKA components and natural knee structures. It is expected that the DOE data will not have the same spread as the anatomic data.

References

- [1] A. A. Amis and D. Eng, "Current Concepts on Anatomy and Biomechanics of Patellar Stability," *Sports Med. Arthrosc.*, vol. 15, no. 2, pp. 48–56, 2007.
- [2] A. A. Ali *et al.*, "Validation of predicted patellofemoral mechanics in a finite element model of the healthy and cruciate-deficient knee," *J. Biomech.*, vol. 49, no. 2, pp. 302–309, 2016.
- [3] J. Bellemans, "Biomechanics of anterior knee pain," *knee*, vol. 10, no. 2, pp. 123–126, 2003.
- [4] J. A. Feller, A. A. Amis, J. T. Andrish, E. A. Arendt, P. J. Erasmus, and C. M. Powers, "Surgical Biomechanics of the Patellofemoral Joint," *Arthrosc. - J. Arthrosc. Relat. Surg.*, vol. 23, no. 5, pp. 542–553, 2007.
- [5] J. Benvenuti, L. Rakotomanana, P. F. Leyvraz, D. P. Pioletti, J. H. Heegaard, and M. G. Genton, "Displacements of the tibial tuberosity. Effects of the surgical parameters," *Clin. Orthop. Relat. Res.*, no. 343, pp. 224–234, 1997.
- [6] J. J. Elias, J. A. Carrino, A. Saranathan, L. M. Guseila, M. J. Tanaka, and A. J. Cosgarea, "Variations in kinematics and function following patellar stabilization including tibial tuberosity realignment," *Knee Surg. Sports Traumatol. Arthrosc.*, vol. 22, no. 10, pp. 2350–2356, 2014.
- [7] S. Mani, M. S. Kirkpatrick, A. Saranathan, L. G. Smith, A. J. Cosgarea, and J. J. Elias, "Tibial tuberosity osteotomy for patellofemoral realignment alters tibiofemoral kinematics," *Am J Sport. Med.*, vol. 39, no. 5, pp. 1024–1031, 2011.
- [8] A. J. Ramappa, M. Apreleva, F. R. Harrold, P. G. Fitzgibbons, D. R. Wilson, and T. J. Gill, "The Effects of Medialization and Anteromedialization of the Tibial Tubercle on Patellofemoral Mechanics and Kinematics," *Am. J. Sports Med.*, vol. 34, no. 5, pp. 749–756, 2006.
- [9] A. Shirazi-Adi and W. Mesfar, "Effect of tibial tubercle elevation on biomechanics of the entire knee joint under muscle loads," *Clin. Biomech.*, vol. 22, pp. 344–351, 2007.
- [10] H. Dejour, G. Walch, and C. Guier, "Patellar problems Factors of patellar instability : an anatomic radiographic study," *Knee Surg. Sport. Traumatol. Arthrosc.*, vol. 2, pp. 19–26, 1994.
- [11] A. A. Amis, W. Senavongse, and A. M. J. Bull, "Patellofemoral Kinematics during Knee Flexion-Extension : An In Vitro Study," *J. Orthop. Res.*, pp. 2201–2211, 2006.
- [12] S. Shalhoub and L. P. Maletsky, "Variation in patellofemoral kinematics due to changes in quadriceps loading configuration during in vitro testing," *J. Biomech.*, vol. 47, pp. 130–136, 2013.
- [13] K. J. Bozic *et al.*, "The Epidemiology of Revision Total Knee Arthroplasty in the United States," *Clin. Orthop. Relat. Res.*, vol. 468, pp. 45–51, 2010.
- [14] D. F. Dalury, D. L. Pomeroy, R. S. Gorab, and M. J. Adams, "Why are Total Knee Arthroplasties Being Revised ?," *J. Arthroplasty*, vol. 28, no. 8, pp. 120–121, 2013.
- [15] W. C. Schroer *et al.*, "Why Are Total Knees Failing Today ? Etiology of Total Knee Revision in 2010 and 2011," *J. Arthroplasty*, vol. 28, no. 8, pp. 116–119, 2013.

- [16] S. J. Song, R. C. Detch, W. J. Maloney, S. B. Goodman, and J. I. Huddleston III, "Causes of Instability After Total Knee Arthroplasty," *J. Arthroplasty*, vol. 29, pp. 360–364, 2014.
- [17] R. S. Namba, G. Cafri, M. Khatod, M. C. S. Inacio, T. W. Brox, and E. W. Paxton, "Risk Factors for Total Knee Arthroplasty Aseptic Revision," *J. Arthroplasty*, vol. 28, no. 8, pp. 122–127, 2013.
- [18] D. N. Bracey *et al.*, "Effects of patellofemoral overstuffing on knee flexion and patellar kinematics following total knee arthroplasty: a cadaveric study," *Int. Orthop.*, vol. 39, no. 9, pp. 1715–1722, 2015.
- [19] W. Wulff and S. J. Incavo, "The Effect of Patella Preparation for Total Knee Arthroplasty on Patellar Strain: A Comparison of Resurfacing Versus Inset Implants," *J. Arthroplasty*, vol. 15, no. 6, pp. 778–782, 2000.
- [20] M. E. Berend, M. A. Ritter, M. E. Keating, P. M. Faris, and B. M. Crites, "The Failure of all-polyethylene components in total knee replacement," *Clin. Orthop. Relat. Res.*, no. 388, pp. 105–111, 2001.
- [21] V. A. Sakellariou, L. A. Poultsides, Y. Ma, J. Bae, S. Liu, and T. P. Sculco, "Risk Assessment for Chronic Pain and Patient Satisfaction After Total Knee Arthroplasty," *Orthopedics*, vol. 39, no. 1, pp. 55–62, 2016.
- [22] J. H. Newman, C. E. Ackroyd, N. A. Shah, and T. Karachalios, "Should the patella be resurfaced during total knee replacement?," *Knee*, vol. 7, no. 1, pp. 6–12, 2000.
- [23] D. Boyd, F. Ewald, W. Thomas, R. Poss, and C. Sledge, "Long-Term complications after total knee arthroplasty with or without resurfacing of the patella," *J. bone Jt. Surg.*, vol. 75, no. 5, pp. 674–681, 1993.
- [24] A. S. Panni, S. Cerciello, C. Del Regno, A. Felici, and M. Vasso, "Patellar resurfacing complications in total knee arthroplasty," *Int. Orthop.*, vol. 38, pp. 313–317, 2014.
- [25] T. P. Pierce, J. J. Jauregui, J. J. Cherian, R. K. Elmallah, S. F. Harwin, and M. A. Mont, "Is There an Ideal Patellar Thickness Following Total Knee Arthroplasty?," *Orthopedics*, vol. 39, no. 1, pp. 187–193, 2016.
- [26] J. S. B. Koh, S. J. Yeo, B. P. H. Lee, N. N. Lo, K. H. Seow, and S. K. Tan, "Influence of patellar thickness on results of total knee arthroplasty: Does a residual bony patellar thickness of ≤ 12 mm lead to poorer clinical outcome and increased complication rates?," *J. Arthroplasty*, vol. 17, no. 1, pp. 56–61, 2002.
- [27] J. L. Baldwin and C. K. House, "Anatomic dimensions of the patella measured during total knee arthroplasty," *J. Arthroplasty*, vol. 20, no. 2, pp. 250–257, 2005.
- [28] C. K. Fitzpatrick, R. H. Kim, A. A. Ali, L. M. Smoger, and P. J. Rullkoetter, "Effects of resection thickness on mechanics of resurfaced patellae," *J. Biomech.*, vol. 46, no. 9, pp. 1568–1575, 2013.
- [29] J. D. Reuben, C. L. McDonald, P. L. Woodard, and L. J. Hennington, "Effect of patella thickness on patella strain following total knee arthroplasty," *J. Arthroplasty*, vol. 6, no. 3, pp. 251–258, 1991.
- [30] D. T. T. Lie, N. Gloria, A. A. Amis, B. P. H. Lee, S. J. Yeo, and S. M. Chou, "Patellar resection during

- total knee arthroplasty: effect on bone strain and fracture risk," *Knee Surg. Sport. Traumatol. Arthrosc.*, vol. 13, no. 3, pp. 203–208, 2005.
- [31] C.-K. Cheng, N.-K. Yao, H.-C. Liu, and K. Lee, "Influences of configuring changes of the patella on the knee extensor mechanism," *Clin. Biomech.*, vol. 1, no. 2, pp. 2–6, 1996.
- [32] J. Mountney, D. R. Wilson, M. Paice, B. A. Masri, and N. V Greidanus, "The Effect of an Augmentation Patella Prosthesis Versus Patelloplasty on Revision Patellar Kinematics and Quadriceps Tendon Force: An Ex Vivo Study," *J. Arthroplasty*, vol. 23, no. 8, pp. 1219–1231, 2008.
- [33] R. R. Singerman, S. M. Gabriel, C. B. Maheshwer, and J. W. Kennedy, "Patellar Contact Forces With and Without Patellar Resurfacing in Total Knee Arthroplasty," *J. Arthroplasty*, vol. 14, no. 5, pp. 603–609, 1999.
- [34] M. J. Star, K. R. Kaufman, S. E. Irby, and C. W. Colwell, "The Effects of patellar thickness on patellofemoral forces after resurfacing," *Clin. Orthop. Relat. Res.*, no. 322, pp. 279–284, 1996.
- [35] C. S. Oishi, K. R. Kaufman, S. Irby, and C. W. Colwell, "Effects of patellar thickness on compressive shear forces in total knee arthroplasty," *Clin. Orthop. Relat. Res.*, no. 331, pp. 283–290, 1996.
- [36] J. A. Rand, "The patellofemoral joint in total knee arthroplasty," *J. Bone Jt. Surgery-American Vol.*, vol. 76, no. 4, pp. 612–620, 1994.
- [37] H. C. Hsu, Z. P. Luo, J. A. Rand, and K. N. An, "Influence of lateral release on patellar tracking and patellofemoral contact characteristics after total knee arthroplasty," *J. Arthroplasty*, vol. 12, no. 1, pp. 74–83, 1997.
- [38] A. M. Merican, K. M. Ghosh, F. R. Y. Baena, D. J. Deehan, and A. A. Amis, "Patellar thickness and lateral retinacular release affects patellofemoral kinematics in total knee arthroplasty," *Knee Surgery, Sport. Traumatol. Arthrosc.*, vol. 22, pp. 526–533, 2012.
- [39] B. C. Bengs and R. D. Scott, "The Effect of Patellar Thickness on Intraoperative Knee Flexion and Patellar Tracking in Total Knee Arthroplasty," *J. Arthroplasty*, vol. 21, no. 5, pp. 650–655, 2006.
- [40] J. L. Pierson *et al.*, "The effect of stuffing the patellofemoral compartment on the outcome of total knee arthroplasty," *J. Bone Jt. Surgery-American Vol.*, vol. 89A, no. 10, pp. 2195–2203, 2007.
- [41] H. Vandenneucker, L. Labey, J. Victor, J. Vander, S. Kaat, and D. Johan, "Patellofemoral arthroplasty influences tibiofemoral kinematics : the effect of patellar thickness," *Knee Surg. Sport. Traumatol. Arthrosc.*, vol. 22, pp. 2560–2568, 2014.
- [42] C. L. Camp, J. R. Martin, A. J. Krych, M. J. Taunton, L. Spencer-gardner, and R. T. Trousdale, "Resection Technique Does Affect Resection Symmetry and Thickness of the Patella During Total Knee Arthroplasty : A Prospective Randomized Trial," *J. Arthroplasty*, vol. 30, no. 12, pp. 2110–2115, 2015.
- [43] C. L. Camp, A. J. Bryan, J. A. Walker, and R. T. Trousdale, "Surgical Technique for symmetric patellar resurfacing during total knee arthroplasty," *J. Knee Surg.*, vol. 26, no. 4, pp. 281–284, 2013.
- [44] C. Anglin *et al.*, "Determinants of patellar tracking in total knee arthroplasty," *Clin. Biomech.*, vol.

- 23, pp. 900–910, 2008.
- [45] S. Fukagawa, S. Matsuda, H. Mizu-uchi, H. Miura, K. Okazaki, and I. Yukihide, “Changes in patellar alignment after total knee arthroplasty,” *Knee Surg. Sport. Traumatol. Arthrosc.*, vol. 19, pp. 99–104, 2011.
- [46] C. Belvedere *et al.*, “Tibio-femoral and patello-femoral joint kinematics during navigated total knee arthroplasty with patellar resurfacing,” *Knee Surgery, Sport. Traumatol. Arthrosc.*, vol. 22, no. 8, pp. 1719–1727, 2014.
- [47] D. F. Dalury, “Extensor mechanism problems following total knee replacement. Journal of Knee Surgery,” *J. Knee Surg.*, vol. 16, no. 2, pp. 118–122, 2003.
- [48] C. L. Phillips, D. A. T. Silver, P. J. Schranz, and V. Mandalia, “The measurement of patellar height A REVIEW OF THE METHODS OF IMAGING,” *J Bone Jt. Surg [Br]*, vol. 9292, no. 8, pp. 1045–53, 2010.
- [49] R. Narkbunnam and K. Chareancholvanich, “Effect of patient position on measurement of patellar height ratio,” *Arch. Orthop. Trauma Surg.*, vol. 135, pp. 1151–1156, 2015.
- [50] R. P. Grelsamer, “Patella Baja After Total Knee Arthroplasty Is It Really Patella Baja?,” *J. Arthroplasty*, vol. 17, no. 1, pp. 66–69, 2002.
- [51] S. M. Kazemi *et al.*, “Pseudo-Patella Baja after total knee arthroplasty,” *Med. Sci. Monit.*, vol. 17, no. 5, p. CR292–CR296, 2011.
- [52] J. G. Seo *et al.*, “Prevention of pseudo-patella baja during total knee arthroplasty,” *Knee Surgery, Sport. Traumatol. Arthrosc.*, vol. 23, pp. 3601–3606, 2015.
- [53] C. S. Ahmad, S. D. Kwak, G. A. Ateshian, W. H. Warden, R. Steadman, and V. C. Mow, “Effects of Patellar Tendon Adhesion to the Anterior Tibia on Knee Mechanics,” *Am. J. Sports Med.*, vol. 26, no. 5, pp. 715–724, 2017.
- [54] V. M. Goldberg, H. E. Figgie, and M. P. Figgie, “Technical considerations in total knee surgery. Management of patella problems,” *Orthop. Clin. north Am.*, vol. 20, no. 2, pp. 189–199, 1989.
- [55] B. S. R. Ward, M. R. Terk, and C. M. Powers, “Patella Alta : Association with Patellofemoral Alignment and Changes in Contact Area During Weight-Bearing,” *J. Bone Jt. Surgery-American Vol.*, vol. 89, no. 8, pp. 1749–1755, 2007.
- [56] E. Simmons and J. C. Cameron, “Patella alta and recurrent dislocation of the patella,” *Clin. Orthop. Relat. Res.*, no. 274, pp. 265–269, 1992.
- [57] J. W. Martin and L. A. Whiteside, “The influence of joint line position on knee stability after condylar knee arthroplasty,” *Clin. Orthop. Relat. Res.*, no. 259, pp. 146–156, 1990.
- [58] J. Kowalzewski, L. Labey, Y. Chevalier, T. Okon, B. Innocenti, and J. Bellemans, “Does joint line elevation after revision knee arthroplasty affect tibio-femoral kinematics, contact pressure or collateral ligament lengths? An in vitro analysis,” *Arch. Med. Sci.*, vol. 11, no. 2, pp. 311–318, 2015.
- [59] G. J. Emodi, J. J. Callaghan, D. R. Pedersen, and T. D. Brown, “Posterior cruciate ligament function following total knee arthroplasty: the effect of joint line elevation.,” *Iowa Orthop. J.*, vol. 19, no.

319, pp. 82–92, 1999.

- [60] M. T. Yoshii, I. Whiteside, L. A. White, S. E. Milliano, “Influence of prosthetic joint line position on knee kinematics and patellar position.,” *J. Arthroplasty*, vol. 6, no. 2, pp. 169–177, 1991.
- [61] S. Fornalski, M. H. McGarry, C. N. H. Bui, W. C. Kim, and T. Q. Lee, “Biomechanical effects of joint line elevation in total knee arthroplasty,” *Clin. Biomech.*, vol. 27, no. 8, pp. 824–829, 2012.
- [62] N. Bertollo, M. H. Pelletier, and W. R. Walsh, “Relationship between patellar tendon shortening and in vitro kinematics in the ovine stifle joint,” *Proc. Institution Mech. Eng. Part H, J. Eng. Med.*, vol. 227, no. 4, pp. 438–447, 2013.
- [63] S. R. Ward, M. R. Terk, and C. M. Powers, “Influence of patella alta on knee extensor mechanics,” *J. Biomech.*, vol. 38, no. 12, pp. 2415–2422, 2005.
- [64] T. Luyckx, K. Didden, H. Vandenneucker, L. Labey, B. Innocenti, and J. Bellemans, “Is there a biomechanical explanation for anterior knee pain in patients with patella alta? INFLUENCE OF PATELLAR HEIGHT ON PATELLOFEMORAL CONTACT FORCE , CONTACT AREA AND CONTACT PRESSURE,” *J. Bone Jt. Surgery-British Vol.*, vol. 91B, no. 3, pp. 344–350, 2009.
- [65] C. Konig *et al.*, “Joint Line Elevation in Revision TKA Leads to Increased Patellofemoral Contact Forces,” *J. Orthop. Res.*, no. January, pp. 1–5, 2010.
- [66] R. Singerman, D. T. Davy, and V. M. Goldberg, “Effects of patella alta and infera on PF contact forces.pdf,” *J. Biomech.*, vol. 27, no. 8, pp. 1059–1065, 1994.
- [67] R. Singerman, K. G. Heiple, D. T. Davy, and V. M. Goldberg, “Effect of Tibial Component Position on Patellar Strain Following Total Knee Arthroplasty,” *J. Arthroplasty*, vol. 10, no. 5, pp. 651–656, 1995.
- [68] S. R. Ward and C. M. Powers, “The influence of patella alta on patellofemoral joint stress during normal and fast walking,” *Clin. Biomech.*, vol. 19, pp. 1040–1047, 2004.
- [69] A. Jawhar, S. Sohoni, V. Shah, and H. P. Scharf, “Alteration of the patellar height following total knee arthroplasty,” *Arch. Orthop. Trauma Surg.*, vol. 134, no. 1, pp. 91–97, 2014.
- [70] R. S. Laskin, “Joint line position restoration during revision total knee replacement,” *Clin. Orthop. Relat. Res.*, no. 404, pp. 169–171, 2002.
- [71] M. D. Partington, J. Sawhney, C. H. Rorabeck, R. L. Barrack, and J. Moore, “Joint line restoration after revision total knee arthroplasty,” *Clin. Orthop. Relat. Res.*, no. 367, pp. 165–171, 1999.
- [72] J. A. Rand, “Modular augments in revision total knee arthroplasty,” *Clin. Orthop. north Am.*, vol. 29, no. 2, pp. 347–353, 1998.
- [73] T. F. Wyss, A. J. Schuster, P. Munger, D. Pfluger, and U. Wehrli, “Does total knee joint replacement with the soft tissue balancing surgical technique maintain the natural joint line?,” *Arch. Orthop. Trauma Surg.*, vol. 126, pp. 480–486, 2006.
- [74] J. Bellemans, “Restoring the joint line in revision TKA : does it matter ?,” *knee*, vol. 11, pp. 3–5, 2004.

- [75] H. E. Figgie, V. M. Goldberg, K. G. Heiple, H. S. Moller, and N. H. Gordon, "The influence of tibial-patellofemoral location on function of the knee in patients with the posterior stabilized condylar knee prosthesis.," *J. bone Jt. Surg.*, vol. 68, no. 7, pp. 1035–1040, 1986.
- [76] M. R. Cope, B. S. O'Brien, and A. M. Nanu, "The Influence of the Posterior Cruciate Ligament in the Maintenance of Joint Line in Primary Total Knee Arthroplasty A Radiologic Study," *J. Arthroplasty*, vol. 17, no. 2, pp. 206–208, 2002.
- [77] A. J. Porteous, M. A. Hassaballa, and J. H. Newman, "Does the joint line matter in revision total knee replacement?," *J. Bone Jt. Surgery-British Vol.*, vol. 90, no. 7, pp. 879–884, 2008.
- [78] J. A. Feller, "Distal realignment (tibial tuberosity transfer).," *Sports Med. Arthrosc.*, vol. 20, no. 3, pp. 152–161, 2012.
- [79] P. Neyret, A. H. N. Robinson, B. Le Coultre, C. Lapra, and P. Chambat, "Patellar tendon length - the factor in patellar instability?," *Knee*, vol. 9, pp. 3–6, 2002.
- [80] W. Guido, H. Christian, H. Elmar, A. Elisabeth, and F. Christian, "Treatment of patella baja by a modified Z - plasty," *Knee Surgery, Sport. Traumatol. Arthrosc.*, vol. 24, no. 9, pp. 2943–2947, 2016.
- [81] J. H. Caton and D. Dejour, "Tibial tubercle osteotomy in patello-femoral instability and in patellar height abnormality," *Int. Orthop.*, vol. 34, no. 2 SPECIAL ISSUE, pp. 305–309, 2010.
- [82] M. J. Hall and V. I. Mandalia, "Tibial tubercle osteotomy for patello-femoral joint disorders," *Knee Surgery, Sport. Traumatol. Arthrosc.*, vol. 24, no. 3, pp. 855–861, 2016.
- [83] J. Bellemans, "Anteromedial tibial tubercle transfer in patients with chronic anterior knee pain and a subluxation-type patellar malalignment.," *Am. J. Sports Med.*, vol. 25, no. 3, pp. 375–381, 1997.
- [84] Y. S. Lee, S. B. Lee, W. S. Oh, Y. E. Kwon, and B. K. Lee, "Changes in patellofemoral alignment do not cause clinical impact after open-wedge high tibial osteotomy," *Knee Surgery, Sport. Traumatol. Arthrosc.*, vol. 24, pp. 129–133, 2016.
- [85] M. A. Vives-Barquiel *et al.*, "Proximalize osteotomy of tibial tuberosity (POTT) as a treatment for stiffness secondary to patella baja in total knee arthroplasty (TKA)," *Arch. Orthop. Trauma Surg.*, vol. 135, no. 10, pp. 1445–1451, 2015.
- [86] J. J. Elias, J. A. Cech, D. M. Weinstein, and A. J. Cosgrea, "Reducing the Lateral Force Acting on the Patella Does Not Consistently Decrease Patellofemoral Pressures," *Am. J. Sports Med.*, vol. 32, no. 5, pp. 1202–1208, 2004.
- [87] P. R. Beck, A. L. Thomas, J. Farr, P. B. Lewis, and B. J. Cole, "Trochlear Contact Pressures After Anteromedialization of the Tibial Tubercle," *Am. J. Sports Med.*, vol. 33, no. 11, pp. 1710–1715, 2005.
- [88] R. Kuroda, H. Kambic, A. Valdevit, and J. T. Andrish, "Articular Cartilage Contact Pressure after Tibial Tuberosity Transfer: A Cadaveric Study," *Am. J. Sports Med.*, vol. 29, no. 4, pp. 403–409, 2001.

- [89] T. Muneta, H. Yamamoto, T. Ishibashi, S. Asahina, and K. Furuya, "Computerized tomographic analysis of tibial tubercle position in the painful female patello femoral joint.," *Am. J. Sports Med.*, vol. 22, no. 1, pp. 67–71, 1994.
- [90] J. M. Stephen, P. Lumpaopong, A. L. Dodds, A. Williams, and A. a Amis, "The effect of tibial tuberosity medialization and lateralization on patellofemoral joint kinematics, contact mechanics, and stability.," *Am. J. Sports Med.*, vol. 43, no. 1, pp. 186–94, 2015.
- [91] P. Aglietti, R. Buzzi, P. De Biase, and F. Giron, "Surgical treatment of recurrent dislocation of the patella," *Clin. Orthop. Relat. Res.*, vol. 308, pp. 8–17, 1994.
- [92] R. Stagni, S. Fantozzi, F. Catani, and A. Leardini, "Can Patellar Tendon Angle reveal sagittal kinematics in total knee arthroplasty ?," *Knee Surg. Sport. Traumatol. Arthrosc.*, vol. 18, pp. 949–954, 2010.
- [93] Y. Mizuno *et al.*, "Q-angle influences tibiofemoral and patellofemoral kinematics," *J. Orthop. Res.*, vol. 19, pp. 834–840, 2001.
- [94] L. Lorin *et al.*, "In Vitro Experimental Testing of the Human Knee : A Concise Review," *J. Knee Surg.*, vol. 29, no. 2, pp. 138–148, 2016.
- [95] L. G. Sutton, F. W. Werner, H. Haider, T. Hamblin, and J. J. Clabeaux, "In vitro response of the natural cadaver knee to the loading profiles specified in a standard for knee implant wear testing," *J. Biomech.*, vol. 43, no. 11, pp. 2203–2207, 2010.
- [96] M. A. Verstraete and J. Victor, "Possibilities and limitations of novel in-vitro knee simulator," *J. Biomech.*, pp. 1–6, 2015.
- [97] P. S. Walker, Y. Heller, and D. J. Cleary, "Preclinical Evaluation Method for Total Knees Designed to Restore Normal Knee Mechanics," *J. Arthroplasty*, vol. 26, no. 1, pp. 152–160, 2011.
- [98] G. Bergmann *et al.*, "Standardized Loads Acting in Knee Implants," *PLoS One*, vol. 9, no. 1, pp. 1–12, 2014.
- [99] T. M. Guess and L. P. Maletsky, "Computational modeling of a dynamic knee simulator for reproduction of knee loading," *J. Biomech. Eng.*, vol. 127, pp. 1216–1221, 2005.
- [100] W. M. Eboch, "A Neural Network Approach to Physiological Joint Loading Profile Generation in the Kansas Knee Simulator," 2015.
- [101] L. P. Maletsky and B. M. Hillberry, "Using a Five-Axis Knee Simulator," *J. Biomech. Eng.*, vol. 127, pp. 123–133, 2005.
- [102] F. G. Fitzwater, "QUANTIFYING THE EFFECT OF SAGITTAL PLANE LOADING ON ANTERIOR-POSTERIOR AND COMPRESSIVE KNEE LOADS DURING DYNAMIC SIMULATIONS," 2014.
- [103] L. P. Maletsky, J. Sun, and N. A. Morton, "Accuracy of an optical active-marker system to track the relative motion of rigid bodies," *J. Biomech.*, vol. 40, pp. 682–685, 2007.
- [104] E. S. Grood and W. J. Suntay, "A Joint Coordinate System for the Clinical Description of three-dimensional motions: Application to the knee," *J. Biomech. Eng.*, vol. 105, pp. 136–144, 1983.

- [105] A. M. J. Bull, M. V Katcburian, Y.-F. Shih, and A. A. Amis, "Standardisation of the description of patellofemoral motion and comparison between different techniques," *Knee Surgery, Sport. Traumatol. Arthrosc.*, vol. 10, pp. 184–193, 2002.
- [106] N. M. Lenz, "SIMULATION OF A NON-CONTACT CUTTING MANEUVER TO GENERATE A REALISTIC ACL Injury in Vitro," 2006.
- [107] T. Schwenke, D. Orozco, E. Schneider, and M. A. Wimmer, "Differences in wear between load and displacement control tested total knee replacements," *Wear*, vol. 267, pp. 757–762, 2009.
- [108] S. Yeh and P. Hsu, "Theory and Applications of the Robust Cross-Coupled Control Design," *J. Dyn. Syst. Meas. Control*, vol. 121, no. September 1999, pp. 524–530, 1999.
- [109] E. Ulu, M. Cakmakci, and N. G. Ulu, "Learning Based Cross-Coupled Control for Multi-Axis High Precision Positioning Systems," in *ASME 2102 5th Annual dynamic Systems and control conference*, 2012, pp. 1–7.
- [110] C.-C. Lo, "An Improved Algorithm for Cross-," *J. Manuf. Sci. Eng.*, vol. 121, no. AUGUST 1999, pp. 537–540, 1996.